The Astronomical Journal, 148:124 (26pp), 2014 December doi:10.1088/0004-6256/148/6/124

HERschel KEY PROGRAM HERITAGE: A FAR-INFRARED SOURCE CATALOG FOR THE MAGELLANIC CLOUDS

Jonathan P. Seale[1,2], Margaret Meixner[1,2], Marta Sewiło[1], Brian Babler[3], Charles W. Engelbracht[4,5], Karl Gordon[2], Sacha Hony[6], Karl Misselt[4], Edward Montiel[4,8], Koryo Okumura[6], Pasquale Panuzzo[6,7], Julia Roman-Duval[2], Marc Sauvage[6], Martha L. Boyer[9], C.-H. Rosie Chen[10], Remy Indebetouw[11,12], Mikako Matsuura[13], Joana M. Oliveira[14], Sundar Srinivasan[15,16], Jacco Th. van Loon[14], Barbara Whitney[3], and Paul M. Woods[17]

[1] The Johns Hopkins University, Department of Physics and Astronomy, 366 Bloomberg Center, 3400 N. Charles Street, Baltimore, MD 21218, USA
[2] Space Telescope Science Institute, 3700 San Martin Drive, Baltimore, MD 21218, USA
[3] Department of Astronomy, 475 North Charter St., University of Wisconsin, Madison, WI 53706, USA
[4] Steward Observatory, University of Arizona, 933 North Cherry Ave., Tucson, AZ 85721, USA
[5] Raytheon Company, 1151 East Hermans Road, Tucson, AZ 85756, USA
[6] CEA, Laboratoire AIM, Irfu/SAp, Orme des Merisiers, F-91191 Gif-sur-Yvette, France
[7] CNRS, Observatoire de Paris-Lab. GEPI, Bat. 11, 5, place Jules Janssen, F-92195 Meudon CEDEX, France
[8] Louisiana State University, Department of Physics & Astronomy, 233-A Nicholson Hall, Tower Dr., Baton Rouge, LA 70803-4001, USA
[9] Observational Cosmology Laboratory, Code 665, NASA Goddard Space Flight Center, Greenbelt, MD 20771, USA
[10] Max-Planck-Institut für Radioastronomie, Auf dem Hügel 69, D-53121 Bonn, Germany
[11] National Radio Astronomy Observatory, 520 Edgemont Road Charlottesville, VA 22903, USA
[12] Department of Astronomy, University of Virginia, P.O. Box 3818, Charlottesville, VA 22903-0818, USA
[13] Department of Physics and Astronomy, University College London, Gower Street, London WC1E 6BT, UK
[14] School of Physical & Geographical Sciences, Lennard-Jones Laboratories, Keele University, Staffordshire ST5 5BG, UK
[15] UPMC-CNRS UMR7095, Institute d'Astrophysique de Paris, F-75014 Paris, France
[16] Academia Sinica, Institute of Astronomy and Astrophysics, P.O. Box 23-141, Taipei 10617, Taiwan
[17] Astrophysics Research Centre, School of Mathematics and Physics, Queen's University Belfast, Belfast BT7 1NN, UK
Received 2014 February 6; accepted 2014 July 2; published 2014 November 7

ABSTRACT

Observations from the *HERschel* Inventory of the Agents of Galaxy Evolution (HERITAGE) have been used to identify dusty populations of sources in the Large and Small Magellanic Clouds (LMC and SMC). We conducted the study using the HERITAGE catalogs of point sources available from the *Herschel* Science Center from both the Photodetector Array Camera and Spectrometer (PACS; 100 and 160 μm) and Spectral and Photometric Imaging Receiver (SPIRE; 250, 350, and 500 μm) cameras. These catalogs are matched to each other to create a *Herschel* band-merged catalog and then further matched to archival *Spitzer* IRAC and MIPS catalogs from the *Spitzer* Surveying the Agents of Galaxy Evolution (SAGE) and SAGE-SMC surveys to create single mid- to far-infrared (far-IR) point source catalogs that span the wavelength range from 3.6 to 500 μm. There are 35,322 unique sources in the LMC and 7503 in the SMC. To be bright in the FIR, a source must be very dusty, and so the sources in the HERITAGE catalogs represent the dustiest populations of sources. The brightest HERITAGE sources are dominated by young stellar objects (YSOs), and the dimmest by background galaxies. We identify the sources most likely to be background galaxies by first considering their morphology (distant galaxies are point-like at the resolution of *Herschel*) and then comparing the flux distribution to that of the *Herschel* Astrophysical Terahertz Large Area Survey (ATLAS) survey of galaxies. We find a total of 9745 background galaxy candidates in the LMC HERITAGE images and 5111 in the SMC images, in agreement with the number predicted by extrapolating from the ATLAS flux distribution. The majority of the Magellanic Cloud-residing sources are either very young, embedded forming stars or dusty clumps of the interstellar medium. Using the presence of 24 μm emission as a tracer of star formation, we identify 3518 YSO candidates in the LMC and 663 in the SMC. There are far fewer far-IR bright YSOs in the SMC than the LMC due to both the SMC's smaller size and its lower dust content. The YSO candidate lists may be contaminated at low flux levels by background galaxies, and so we differentiate between sources with a high ("probable") and moderate ("possible") likelihood of being a YSO. There are 2493/425 probable YSO candidates in the LMC/SMC. Approximately 73% of the *Herschel* YSO candidates are newly identified in the LMC, and 35% in the SMC. We further identify a small population of dusty objects in the late stages of stellar evolution including extreme and post-asymptotic giant branch, planetary nebulae, and supernova remnants. These populations are identified by matching the HERITAGE catalogs to lists of previously identified objects in the literature. Approximately half of the LMC sources and one quarter of the SMC sources are too faint to obtain accurate ample FIR photometry and are unclassified.

Key words: circumstellar matter – galaxies: dwarf – infrared: stars – Magellanic Clouds – stars: formation – stars: pre-main sequence

Online-only material: color figures

1. INTRODUCTION

Dust emission is a useful tracer of non-stellar baryonic matter, and can therefore provide key insights into the process by which the interstellar medium (ISM) is converted into stars and then returned to the ISM in stellar outflows or following the stars' deaths. Infrared (IR) emission from warmed dust in and around the objects that mediate this process—forming and dying stars—can therefore be an important observable in understanding the life cycle of baryonic matter within galaxies.

In this paper we use data from the *Herschel Space Observatory* (Pilbratt et al. 2010) Key Project *Herschel* Inventory of the Agents of Galaxy Evolution (HERITAGE; Meixner et al. 2013) to identify such dusty objects in the Large and Small Magellanic Clouds (LMC and SMC; collectively referred to as the Magellanic Clouds, MCs). HERITAGE is a uniform far-infrared (far-IR) survey of the MCs that imaged the entirety of the galaxies at 100, 160, 250, 350, and 500 μm. The MCs are excellent astrophysical laboratories to study the life cycle of baryonic matter, as their proximity ($\sim$50 and 60 kpc for the LMC and SMC, respectively; Ngeow & Kanbur 2008; Szewczyk et al. 2009) permits a detailed study of the point source populations on galaxy-wide scales. Since all sources within a single MC are at nearly the same distance, source luminosities can be reliably determined and their relative luminosities are even more robust. In particular, the thin disk morphology and nearly face-on orientation of the LMC makes interpretation fairly straightforward. A filament of primarily atomic gas, called the Magellanic Bridge, joins the two MCs over some 15 kpc (Subramanian & Subramaniam 2009, 2010, 2012). The densest part of the Bridge is nearest the SMC and is typically called the Tail (e.g., Muller et al. 2003; Gordon et al. 2009). With signs of on going star formation (Chen et al. 2014; Sewiło et al. 2013), the Tail is included in our observations and mosaicked together with the SMC.

FIR emission is dominated by thermal emission from dust. Point sources emitting at these wavelengths have both significant circumstellar dust and a source of radiation to heat that dust. Such objects represent the transitional stages between stars and the ISM. Since star formation occurs in the densest regions of molecular clouds, dust is an excellent tracer of young stellar objects (YSOs) still surrounded by their natal material (see review by Evans 1999). Large survey areas are needed to identify statistically significant populations of forming stars, and a number of recent IR surveys have been used to identify the sites of star formation over large regions of the Milky Way (MW). Large observing programs utilizing the *Spitzer Space Telescope* (Werner et al. 2004) imaged the Galactic plane between longitudes of $0° < l < 63°$ and $298° < l < 360°$ at 3.6, 4.5, 5.8, and 8.0 μm (GLIMPSE; Churchwell et al. 2009), and later at 24 and 70 μm (MIPSGAL; Carey et al. 2009). Most recently, Hi-GAL (The *Herschel* infrared Galactic Place Survey; Molinari et al. 2010) extended the wavelength coverage into the FIR with *Herschel* by imaging the entire Galactic plane with $|b| < 1°$.

Nearby low-mass YSOs were readily detected in the *Spitzer* images, but one of the primary science drivers of the GLIMPSE, MIPSGAL, and Hi-GAL surveys was to identify the more distant high-mass protostar population in the inner Galactic disk (e.g., Cyganowski et al. 2008; Elia et al. 2010; Battersby et al. 2011). Hundreds of massive YSOs were first identified in the *Spitzer* images (e.g., Cyganowski et al. 2008), and the later inclusion of *Herschel* data allowed for nearly complete wavelength coverage for early stage YSOs' spectral energy distributions (SEDs). Integrating over the SEDs measures the sources' bolometric luminosities (e.g., Elia et al. 2010), and fitting the FIR photometry to graybodies estimates the dust temperature of the YSOs' envelopes (e.g., Veneziani et al. 2013). The *Herschel* observations also revealed a colder population of starless, dusty ISM clumps (e.g., Battersby et al. 2011; Veneziani et al. 2013) not detected by *Spitzer* that could be the pre-stellar precursors to YSOs.

Even maps of the entire Galactic plane—which are very costly in telescope time—cannot sample an entire galaxy due to confusion and screening of sources on the far side of the MW. The MCs hold a distinct advantage as they can be imaged in their entirety with a reasonable amount of telescope time at a spatial resolution sufficient to resolve stellar populations. Statistical studies can then constrain the timescales for these populations, most notably those associated with star formation.

HERITAGE is comparable in scale and scope to the large *Herschel* surveys of the MW such as Hi-GAL, HOBYS (*Herschel* imaging survey of OB YSOs; Motte et al. 2010), and the *Herschel* Gould Belt Survey (André et al. 2010). Indeed, objects and structures found in the HERITAGE data are comparable to those detected in these MW *Herschel* surveys. In particular, we note the presence of filamentary structure in the MCs within which many of the FIR point sources are located, reminiscent of the ubiquitous filamentary structure seen in the Galaxy (e.g., Molinari et al. 2010; Hill et al. 2011). The point sources in these surveys are dominated by those associated with star formation: pre-stellar cores and YSOs. These populations dominate the HERITAGE observations as well (Sewiło et al. 2010), but differences in spatial resolution make a direct comparison difficult. At the distance of the MCs, *Herschel* has a spatial resolution of at best 2 pc, meaning blending of clustered sources is prevalent.

The difference in distance (and resulting spatial resolution) between MW and MC star formation regions presents the need for caution when comparing their YSO populations. The nearest Galactic low-mass star formation regions are on the order of hundreds of times closer than the MCs. High-mass star formation is rarer, and so the closest MW regions in which it occurs are correspondingly farther, but still several tens of times closer than the MCs. The result is that MC YSO surveys are not sensitive to the least massive YSOs, and small clusters of sources (cluster diameters less than $\sim$1 pc) can be unresolved and blended into a single source. Indeed, higher resolution observations from instruments such as the *Hubble Space Telescope* reveal many of these MC YSOs to be clusters of sources whose luminosities are typically dominated by one or several high-luminosity YSOs (e.g., Chen et al. 2009; Carlson & Meixner 2011; Sewiło et al. 2013; Walborn & Barbá 2013). For this reason, it is important to remember that sources identified as MC YSOs both here and in the literature may be separated with improved resolution into a small cluster of YSOs.

MC YSOs have been previously surveyed in the mid-IR *Spitzer* SAGE (Surveying the Agents of Galaxy Evolution; Meixner et al. 2006) and SAGE-SMC (SAGE in the Tidally Stripped, Low Metallicity SMC; Gordon et al. 2011) surveys. Imaging the LMC and SMC over the full *Spitzer* wavelength range (3.6–160 μm), the SAGE surveys were sensitive to warm ($\sim$100 K) dust and used to identify thousands of YSO candidates (e.g., Whitney et al. 2008; Gruendl & Chu 2009; Sewiło et al. 2013).

A preliminary study by Sewiło et al. (2010) identified 210 candidate YSOs in a 2° × 8° strip of the LMC using the HERITAGE science demonstration phase data. The work presented in this paper builds upon this previous *Spitzer* and *Herschel* work by extending the survey to the entire HERITAGE survey area. Operating at longer wavelengths, *Herschel* is sensitive to lower dust temperatures than *Spitzer*, meaning it detects a different yet overlapping population of sources. Radiative transfer models, such as those presented by Whitney et al. (2003), show how the SED of a YSO evolves with time. In the earliest stages of evolution, it is dominated by the FIR, because the young YSO is deeply embedded within a circumstellar envelope that absorbs the forming star's photospheric emission, warms its dust to the order of tens of degrees Kelvin, and re-emits it in the FIR. In time, the envelope dissipates, revealing the warmer inner parts of the envelope and a circumstellar disk radiating in the near- and mid-IR. The SEDs of these later stages are dominated by the emission blueward of the FIR; such a source may be detectable by *Spitzer* but not *Herschel*. Together, *Spitzer* and *Herschel* provide nearly compete spectral coverage for most early stage forming stars.

By comparison, there is a relatively small population of evolved stars that are bright at *Herschel* wavelengths, namely some red supergiants (RSGs; Boyer et al. 2010), asymptotic giant branch (AGB) stars, post-AGBs, planetary nebulae (PNs), and supernova remnants (SNRs; Otsuka et al. 2010). AGB stars are shedding material that condenses into dust, returning it to the ISM in shell-like structures formed by stellar pulsations (see review by Iben & Renzini 1983). Early during this process, these shells lie close to the star (Mattsson et al. 2007), have high dust temperatures, and are consequently bright in the near- and mid-IR. Indeed, tens of thousands of dusty evolved stars were identified in the *Spitzer* SAGE and SAGE-SMC images (e.g., Srinivasan et al. 2009; Boyer et al. 2011; Riebel et al. 2012). As the shells expand to larger radii, they are heated to lower temperatures and become redder (Habing 1996; Mattsson et al. 2007). Late stage, very dusty, red AGBs, the so-called extreme AGBs, can be detected in the FIR (e.g., Groenewegen et al. 2011). The ejected material will eventually form a PN, with post-AGBs bridging the AGB and PN stages. More massive stars die in supernova (SN) explosions, and FIR emission from SNR dust that forms in the ejecta has been detected, including in the LMC SNR SN 1987 A (e.g., Matsuura et al. 2011). Finally, because galaxies as a whole are amalgamations of the above stellar populations and ISM dust emission, distant galaxies typically appear as point sources in *Herschel* images (Eales et al. 2010). It is a primary goal of this paper to separate the MC point sources detected in HERITAGE into these different categories.

In this paper we characterize thousands of FIR bright objects identified in the MCs with HERITAGE. The brightest objects are dominated by YSOs, and the dimmest by background galaxies and dusty, possibly starless clumps of the ISM. We also identify a smaller population of stars in very dusty, late stages of evolution (extreme AGBs, post-AGBs, PNs, SNRs). In Section 2, we describe the observations used in the study. Section 3 outlines the properties of the HERITAGE catalogs of point sources, Section 4 details our classification method, and Section 5 contains a discussion of the properties of the classified sources. A summary of the results can be found in Section 6.

Table 1
SAGE and HERITAGE Image Angular Resolutions

Wavelength (μm)	Instrument	FWHM ($''$)	FWHM ($''$)
		LMC	SMC
3.6	*Spitzer* IRAC	1.7	1.7
4.5	*Spitzer* IRAC	1.7	1.7
5.8	*Spitzer* IRAC	1.9	1.9
8.0	*Spitzer* IRAC	2	2
24	*Spitzer* MIPS	6	6
70	*Spitzer* MIPS	18	18
160	*Spitzer* MIPS	40	40
100	*Herschel* PACS	8.6	8.8
160	*Herschel* PACS	12.6	12.6
250	*Herschel* SPIRE	18.3	18.3
350	*Herschel* SPIRE	26.7	26.7
500	*Herschel* SPIRE	40.5	39.7

2. *HERSCHEL* HERITAGE OBSERVATIONS AND SOURCE EXTRACTION

The present paper uses FIR observations obtained by the European Space Agency (ESA) *Herschel Space Observatory* (Pilbratt et al. 2010) as part of the key project HERITAGE (Meixner et al. 2013), which mapped the Magellanic System at 100, 160, 250, 350, and 500 μm with the Spectral and Photometric Imaging Receiver (SPIRE; Griffin et al. 2010) and Photodetector Array Camera and Spectrometer (PACS; Poglitsch et al. 2010). For brevity, we refer to the PACS 100 and 160 μm data as P100 and P160, and the SPIRE 250, 350, and 500 μm data as S250, S350, and S500, respectively. Utilizing 285 hours of observing time, HERITAGE covered the LMC (8° × 8.5°), the SMC (5° × 5°), and a 4° × 3° region of the SMC Tail at two different epochs, which were then combined during data reduction. The observations of the Tail were mosaicked with the SMC, and will here be referred to collectively as the SMC. For further information regarding the observing strategy and image generation, see the HERITAGE data overview paper by Meixner et al. (2013).

The angular resolution of the HERITAGE images is a function of wavelength, and Table 1 documents the FWHM of each waveband's point-spread function (PSF), as measured directly from the images (Meixner et al. 2013). P100 achieves the highest resolution of $8\farcs6 - 8\farcs8$, 2–3 pc at the distances of the MCs. By contrast, the S500 image's PSF has nearly five times the FWHM.

2.1. HERITAGE Point Source Catalogs

We use the HERITAGE point source catalogs from Meixner et al. (2013), which were extracted from mosaicked images combining two epochs of observations. For each band and galaxy, Meixner et al. (2013) released a subsample of the full list of point sources extracted from the images, which contained only the most reliable point sources. These high reliability lists, called the HERITAGE Catalogs, contain the positions, fluxes, flux uncertainties, and other photometric parameters for *Herschel*-detected point sources in the MCs; there is one catalog per band (P100, P160, S250, S350, S500) and galaxy (LMC and SMC). Source fluxes were extracted using the PSF-fitting software StarFinder (Diolaiti et al. 2000), and flux uncertainties were estimated to reflect the multiple sources of uncertainty including the complex background, PSF

Table 2
Cross-Band Matching

Image	Number of Sources in Catalog	Number of Objects Detected in Other Herschel Images					Fraction in No Other Images	Fraction in ⩾3 Images
		P100	P160	S250	S350	S500		
				LMC				
PACS 100	4164	⋯	3511	2990	2281	1432	0.09	0.76
PACS 160	9324	3393	⋯	7518	5329	3165	0.08	0.68
SPIRE 250	25,445	2766	6928	⋯	16,527	6731	0.22	0.36
SPIRE 350	22,082	2011	4517	15,595	⋯	7044	0.21	0.35
SPIRE 500	7355	1094	2236	5274	6482	⋯	0.07	0.70
				SMC				
PACS 100	898	⋯	798	794	655	298	0.04	0.90
PACS 160	1590	775	⋯	1420	1052	406	0.04	0.76
SPIRE 250	5465	748	1355	⋯	3690	859	0.24	0.30
SPIRE 350	5313	588	940	3612	⋯	1058	0.26	0.27
SPIRE 500	1069	224	292	735	1011	⋯	0.04	0.68

Table 3
Band-Merged Catalog Properties

Galaxy	Number of Objects	Fraction in One Image	Fraction in Two Images	Fraction in Three Images	Fraction in Four Images	Fraction in Five Images
LMC	35,323	0.34	0.37	0.19	0.07	0.03
SMC	7503	0.38	0.39	0.14	0.07	0.03

Table 4
Object Group Statistics

Galaxy	Number of Objects	Number of Groups	Smallest Group Size	Largest Group Size	Average Group Size
LMC	35,323	2700	2	6	2.2
SMC	7503	254	2	5	2.3

shape, and goodness of fit. Typical flux uncertainties are on the order of 5%–20%. For a more detailed discussion of the source extraction process, its merits, and its limitations see Meixner et al. (2013). The catalogs are publicly available from the *Herschel* Science Archive.[18]

2.2. Cross-Band Matching and Groups of Sources

To identify astronomical objects that are detected in multiple HERITAGE images, we positionally cross-matched each galaxy's five HERITAGE catalogs (P100, P160, S250, S350, and S500) with each other. We adopt a matching distance of $0.7 \times \mathrm{FWHM_{max}}$ (which contains ∼99% of inter-band matches within $2 \times \mathrm{FWHM_{max}}$), where $\mathrm{FWHM_{max}}$ is the largest of the two matching catalogs' FWHMs (see Table 1). This fairly large matching radius is required because real positional offsets are expected; many of the catalogs' point sources are local density and brightness enhancements embedded within larger ISM structures, and different *Herschel* wavelengths can trace different parts of that structure, resulting in real, measurable positional offsets. In the rare case that one source from the higher resolution image is matched to more than one source in the longer wavelength image, the closest match is adopted. If there is more than one higher resolution match to a lower resolution source, only sources within $0.5 \times \mathrm{FWHM_{max}}$ or—if no source is within $0.5 \times \mathrm{FWHM_{max}}$—within 150% of the closest distance are kept. The latter criterion ensures that only sources associated with the same astronomical object are matched. Table 2 documents the number of images in which each catalog's sources are detected. Note that in both the LMC and SMC, a majority of P100, P160, and S500 catalog sources are coincident with two or more sources detected in other wavebands. This is in contrast with the S250 and S350 catalogs, a majority of which are coincident with sources in one or no other wavebands. The HERITAGE SPIRE observations are more sensitive than PACS (Meixner et al. 2013), so many sources near the sensitivity limit are detected in only the highest angular resolution SPIRE images, S250 and S350.

After completion of the matching, individual astronomical objects—which are identified in 1–5 HERITAGE images—are assigned a unique name. Source naming convention is an 11 character string, HSOBMHERICC, followed by a source-specific postion designation JRR.RRRRSDD.DDDD. In the string, HSO denotes the *Herschel Space Observatory*; band-matched (BM) specifies the instrument and the wavelength (in this case BM, for band-matched); HERI is a four-character code for the HERITAGE project; the first C denotes the epoch

[18] www.cosmos.esa.int/web/herschel/science-archive

Table 5
Band-Matched Catalogs'[a] Contents

Column	Name	Description	Null
1	SourceName	The identifying name of the source[b]	···
2	R.A.(J2000)	Right Ascension, J2000 (deg)	···
3	Decl.(J2000)	Declination, J2000 (deg)	···
4	GroupID	Running identification number specifying group membership	–999
5	Dominant	1 for dominant source, 0 for not	–999
6	PointFlag	1 for point-like, 0 for not	···
6	P100Name	P100 source name as given in the HERITAGE catalogs	–999
7	P160Name	P160 source name as given in the HERITAGE catalogs	–999
8	S250Name	S250 source name as given in the HERITAGE catalogs	–999
9	S350Name	S350 source name as given in the HERITAGE catalogs	–999
10	S500Name	S500 source name as given in the HERITAGE catalogs	–999
11	f100	P100 source flux (mJy)	–999
12	u100	P100 source flux uncertainty (mJy)	–999
13	flag100	P100 source flux flag	–999
14	f160	P160 source flux (mJy)	–999
15	u160	P160 source flux uncertainty (mJy)	–999
16	flag160	P160 source flux flag	–999
17	f250	S250 source flux (mJy)	–999
18	u250	S250 source flux uncertainty (mJy)	–999
19	flag250	S250 source flux flag	–999
20	f350	S350 source flux (mJy)	–999
21	u350	S350 source flux uncertainty (mJy)	–999
22	flag350	S250 source flux flag	–999
23	f500	S500 source flux (mJy)	–999
24	u500	S500 source flux uncertainty (mJy)	–999
25	flag500	S250 source flux flag	–999
26	IRACName	SAGE IRAC Designation	–999
27	MIPS24Name	SAGE MIPS 24 μm Designation	–999
28	MIPS70Name	SAGE MIPS 70 μm Designation	–999
29	SHdist	Distance between *Spitzer*24 μm and *Herschel* sources (arcsec)	–999
30	f3.6	3.6 μm source flux (mJy)	–999
31	u3.6	3.6 μm source flux uncertainty (mJy)	–999
32	f4.5	4.5 μm source flux (mJy)	–999
33	u4.5	4.5 μm source flux uncertainty (mJy)	–999
34	f5.8	5.8 μm source flux (mJy)	–999
35	u5.8	5.8 μm source flux uncertainty (mJy)	–999
36	f8.0	8.0 μm source flux (mJy)	–999
37	u8.0	8.0 μm source flux uncertainty (mJy)	–999
38	f24	24 μm source flux (mJy)	–999
39	u24	24 μm source flux uncertainty (mJy)	–999
40	f70	70 μm source flux (mJy)	–999
41	u70	70 μm source flux uncertainty (mJy)	–999

[a] Available from the *Herschel* Science Archive.
[b] A description of source name construction is found in the text.

(combined-epoch), and the second C designates the list type, C for catalog. RR.RRRR and DD.DDDD are the R.A. and decl., respectively, in degrees to four decimal places, and S is the sign of the declination. The position of the source from the shortest wavelength image it is detected in is adopted as the source's position. We call the resulting catalog the Band-Matched Catalog (BMC). Tables 3 and 4 document some statistics of the BMCs for both galaxies. The 73,464/15,091 total point sources in the LMC/SMC HERITAGE Catalogs constitute 35,322/7503 unique BMC sources. For the remainder of the paper, we refer to this Band-Matched Catalog as the BMC, which is available from the *Herschel* Science Archive. Table 5 documents the columns found in the BMCs.

There exists significant variation in angular resolution between the five *Herschel* bands. Point sources in the shorter wavelength, higher resolution images are sometimes separated by distances smaller than the angular resolution of the longer wavelength images, meaning the *Herschel* data—particularly the SPIRE images—can suffer from crowding and source blending. Crowding/blending issues complicate the interpretation of flux measurements of an astronomical source, as the flux extracted by StarFinder may be a summation of multiple objects. This issue is most prevalent in star formation regions, where sources are known to be clustered on size scales near and smaller than the spatial resolution of the observations.

Indeed, we find that some long-wavelength catalog sources are matched to multiple short-wavelength catalog sources such that the point sources in the long-wavelength image are a summation of the flux from multiple short-wavelength sources. To track this possible sharing of flux at some wavelengths between distinct astronomical sources, we have assigned BMC sources that share matches with other sources' group identification (ID) numbers. Group IDs are assigned to sources as a running number ordered by R.A. and then decl., and BMC sources that share a catalog point source from at least a single band all have the same group ID. BMC sources that share a group ID (and therefore share flux in at least one image) are together considered a group of sources. For example sources HSOBMHERICC J72.200191-69.159669 and HSOBMHERICC J72.208295-69.157965 are distinguishable in PACS images, but blend in the SPIRE images into a single source. In the BMC, these two sources have the same S250 and S350 fluxes. They constitute a group and are assigned the same LMC group ID (in this case, 20). Often, the photometry extracted from the longest wavelength, lowest resolution image is dominated by the emission from one source in the group. We define a group's dominant source as the one that is brighter (within the uncertainties) than all other sources in the group at all PACS wavelengths it is detected in, or at SPIRE wavelengths if there is no PACS detection. Groups' dominant sources are indicated in the BMC. Most sources are not blended into groups: of the 35,322/7503 BMC sources in the LMC/SMC, only 17%/8% are in groups. Table 4 documents the statistics of the groups for each galaxy.

2.3. Matching to Spitzer Surveying the Agents of Galaxy Evolution

We have matched the BMC to point sources identified in the mid-IR with *Spitzer* utilizing the point source catalogs from the *Spitzer* Legacy programs SAGE and SAGE-SMC. The programs imaged the galaxies with both the IRAC (3.6, 4.5, 5.8, and 8.0 μm) and MIPS (24, 70, and 160 μm) instruments. We positionally matched the BMC to the SAGE MIPS 24 μm and 70 μm full lists, which include all MIPS sources extracted from the images, available for download along with the data delivery document through the NASA/IPAC Infrared Science Archive.[19,20] A liberal matching distance of 5″ was selected by first matching the BMC to *Spitzer* sources with a large

[19] http://irsa.ipac.caltech.edu/data/SPITZER/SAGE/
[20] http://irsa.ipac.caltech.edu/data/SPITZER/SAGE-SMC/

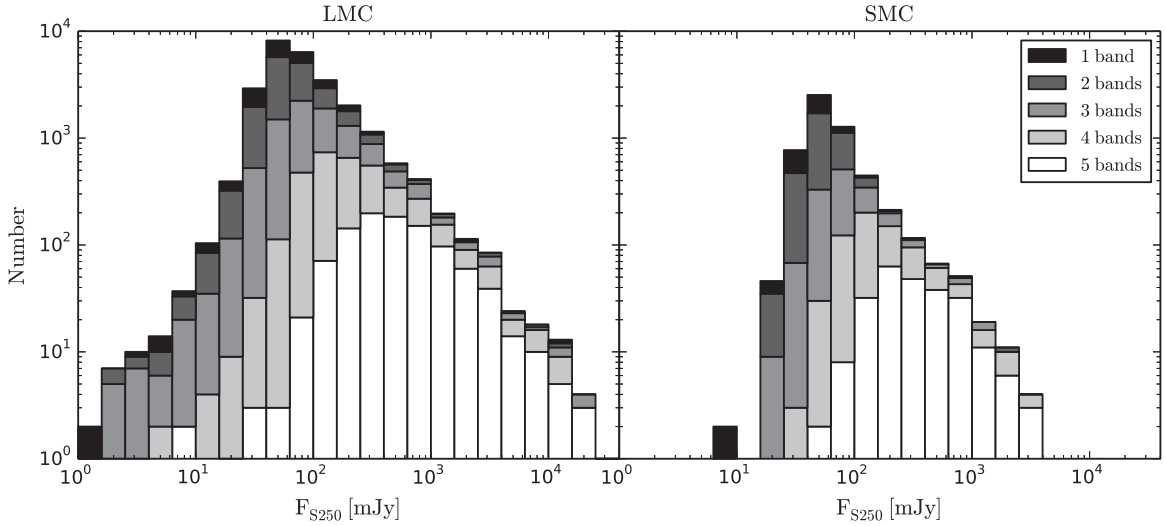

Figure 1. S250 flux distribution of the BMC in the LMC (left) and SMC (right). The shade of the histogram denotes the number of images in which the source was detected. The distributions are skewed to higher fluxes with an increasing number of detected bands, indicating that the fluxes of all the bands tend to scale with each other and that the dimmest sources are detected in the fewest bands.

40″ matching distance, and then adopting as a final value the distance above which the number of matches falls to essentially zero. In cases where sources have multiple matches, only the nearest matches are kept. Because of the large difference in angular resolutions, we did not directly match IRAC source lists to the HERITAGE BMC, but instead bootstrapped the IRAC sources through the MIPS 24 μm matches. SAGE and SAGE-SMC data products include *Spitzer* band-merged catalogs that match MIPS to IRAC sources, so if a BMC source has a MIPS 24 μm match, then the source adopts the photometry of the closest IRAC source within 1.″5 of the MIPS 24 μm source. The *Spitzer* photometry is included in the BMCs.

3. PROPERTIES OF THE HERITAGE BAND-MATCHED CATALOG

3.1. Flux Distribution and Completeness

Figure 1 shows the S250 flux distribution of sources identified in 1, 2, 3, 4, and all 5 bands for both galaxies. Note that as sources are detected in more bands, the flux distribution skews toward higher fluxes. Most objects (>60%) are identified in at least two images, and 29% and 23% of the objects are identified in three or more images in the LMC and SMC, respectively. In both galaxies, only ∼3% of sources are identified in all five *Herschel* images. Because of the lower sensitivity of the PACS observations, objects detected in PACS tend to lie within the brighter portion of the flux distribution, and hence a majority (∼70%) of PACS sources have coincident sources in at least three of the five HERITAGE catalogs.

By contrast, the higher sensitivity SPIRE images contain many sources on the edge of the detection limit. Indeed, of the approximately 1/3 of BMC sources detected in only one band, >90% are SPIRE-only sources. Moreover, ∼1/4 BMC sources are identified only in S250 and S350, the most sensitive of the HERITAGE images (Meixner et al. 2013). These objects are on the faint end of the flux distribution (average S250 flux of ∼100 mJy), and, as will be shown later, many of them are distant background galaxies.

The HERITAGE images are dominated by thermal emission from dust in the ISM, which ranges in measured surface brightness over several orders of magnitude from ∼10 to $>10^3$ MJy sr^{-1} and displays a complex structure of knots and filaments. Many of the point sources are located within and confused with this bright, complex background causing the background emission-dependent flux distribution shown in Figure 2. The top panel shows the S250 flux distribution for LMC sources located on what we label a low background surface brightness, $B_{S250} < 10$ MJy sr^{-1}. The lower panels show the same but for sources in a high background, and each curve shows sources located in a different background interval. The vertical dashed lines mark the peak of the distribution caused by the loss of faint sources at low flux levels. At low background, the peak occurs at ∼40 mJy, and the peak moves to brighter fluxes (to the right) with increasing background levels. In the highest background emission levels in Figure 2, $B_{S250} \geqslant 10^{2.5}$ MJy sr^{-1}, the peak is at ∼2 Jy, such that only the brightest sources are being detected.

Figure 2 demonstrates that the completeness of the BMC depends on the background within which the sources are located and thus varies over the image. The majority of the HERITAGE images have a low surface brightness; in the case of the S250 image, 84% of the LMC and 98% of the SMC have a surface brightness $B_{S250} < 10$ MJy sr^{-1}, meaning the completeness is well-characterized in most of the HERITAGE images. Figure 2 shows that the peak of the flux distribution increases by a factor that of ∼2 from the low background (<10 MJy sr^{-1}) to the $10^{1.5}$ MJy sr$^{-1} \leqslant B_{S250} > 10^2$ MJy sr^{-1} background surface brightness bin. If the position of the peak follows the completeness limit linearly, then the completeness limit varies by only a factor of ∼2 at surface brightnesses below 10^2 MJy sr^{-1}. Less than 0.5% of the LMC S250 image and 0.1% of the SMC S250 image have a background emission brightness more than 10^2 MJy sr^{-1}, meaning the completeness limit varies by only approximately a factor of 2 over the vast majority of the images' area.

The completeness of the BMC differs from the completeness reported in Meixner et al. (2013) for all sources extracted because the HERITAGE catalogs contain only the most reliable

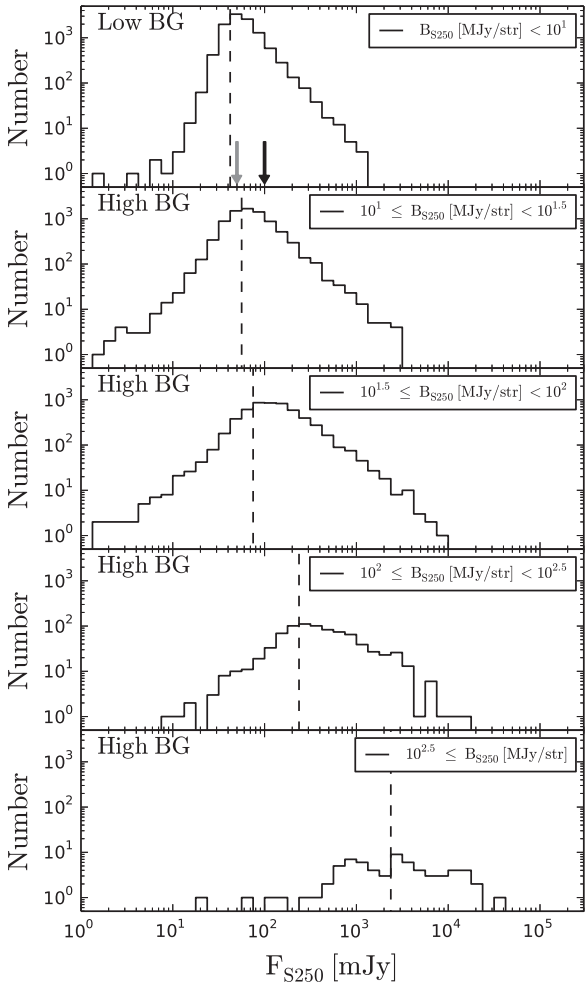

Figure 2. S250 flux distribution of the LMC's BMC. The top panel shows sources located in a low background, while the other panels show high backgrounds that increase in surface brightness from top to bottom as indicated in the legends. In the top panel, the gray arrow marks the 90% completeness limit for all S250 sources extracted from the HERITAGE images (Meixner et al. 2013), while the black arrow indicates the 100% completeness limit for the S250 catalog. In all panels, the dashed, vertical line denotes the peaks of the distributions. The peak of the distribution, and therefore the completeness limit, moves to higher fluxes as the background brightness increases.

subsample of all sources extracted. Details of catalog inclusion can be found in Meixner et al. (2013); false source insertion tests found the P100, P160, S250, S350, and S500 catalogs to be 100% complete in low backgrounds above 500, 200, 100, 200, and 200 mJy, respectively (Meixner et al. 2013). On average, the HERITAGE point sources are nearly colorless at *Herschel* wavelengths, i.e., the ratio of a sources' fluxes at two differing wavelengths is approximately unity. If we adopt this rough approximation that $F_{P100} = F_{P160} = F_{S250} = F_{S350} = F_{S500}$, then the BMC is 100% complete at low background (i.e., sources are detected in *at least* one HERITAGE image) for sources brighter than 100 mJy in any *Herschel* waveband. Figure 2 shows this is clearly not true for sources at the highest backgrounds, however if we assume the completeness increases linearly with the flux distribution peak, then the BMC is complete for sources brighter than ~200 mJy in any single *Herschel* band over the >99% of the HERITAGE image area with a S250 surface brightness, $B_{S250} < 10^2$ MJy sr^{-1}.

3.2. Spatial Distribution

Figure 3 shows the spatial distribution of the BMC sources compared to the galaxies' Hα emission from SHASSA (Southern Hα Sky Survey Atlas; Gaustad et al. 2001) and 250 μm emission (HERITAGE). Most of a galaxy's flux in the FIR is emission from dust in the ISM, not point sources; for all of the *Herschel* wavebands, only 2–7% of the MCs' total flux (reported in Meixner et al. 2013) is accounted for by catalog sources. The bright patches in the 250 μm image correspond to regions with the highest ISM dust (and thus gas) surface density (Meixner et al. 2013). Star formation occurs in many of these high surface density regions, as evidenced by the close coincidence between the Hα and 250 μm emission.

Many of the BMC sources are also positionally coincident with these high surface density regions, implying, as expected, that many of the FIR point sources are objects associated with star formation such as YSOs. The correspondence is stronger for bright sources than dim ones. In Figure 4, we show the spatial distribution of sources as a function of S250 flux; sources detected only in SPIRE are shown in gray, while those detected in at least one PACS band (and possibly SPIRE) are shown in black. These figures reiterate that dim sources are often below the PACS detection limit. While the structure of MC star formation regions is recognizable in every panel, it is most evident for the brightest sources. There is a large population of faint, SPIRE-only sources uncorrelated spatially with MC structures. The spatial distribution of these faint sources implies they are unassociated with the MCs, and are good candidates for background galaxies. We further explore the background galaxy population in Section 4.

4. SOURCE CLASSIFICATION

The brightest objects at *Herschel* wavelengths are the dustiest objects. Forming stars are surrounded by dusty envelopes of gas from which they accrete material, and radiation from the YSOs warms the surrounding medium, making them among the brightest objects at these wavelengths (Evans 1999). Radiative transfer modeling (e.g., Whitney et al. 2013) shows that compact, dusty clumps of gas, even without an embedded source, can be warmed by the interstellar radiation field (ISRF) and appear as FIR point sources. The positional distribution of faint sources seen in Figure 4 suggests there is potentially a large population of background galaxies whose ISM dust emits in the FIR. Finally, stars in an evolved stage of stellar evolution (e.g., extreme AGBs, post-AGBs, PNs, and SNRs) produce dust that can emit in the FIR. We classify the BMC objects into these categories via a two-step process: (1) sources are first matched to catalogs of sources of known classification in the literature; (2) the positions, morphology, and IR photometry of sources are analyzed individually and considered along with their previous classification to determine a likely classification.

4.1. Matching to Previously Classified Sources: The Catalogs

The LMC and SMC have been imaged at many wavelengths, and extensive lists of categorized objects are now available in the literature. We have matched the HERITAGE BMC to some of the more pertinent catalogs available in the literature of the most likely constituents—YSOs, dust clumps, background galaxies, PNs, SNRs, and some other evolved stellar types

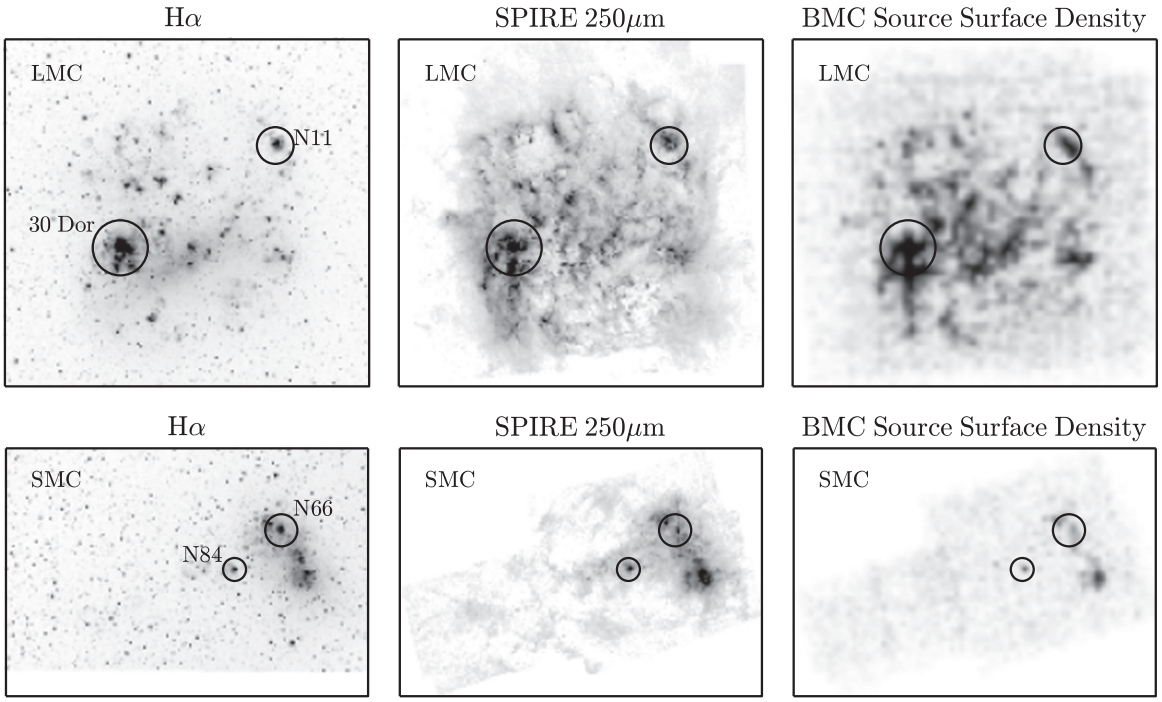

Figure 3. LMC (top row) and SMC (bottom row). Left: SHASSA Hα image; center: HERITAGE 250 μm image; right: surface density of the HERITAGE Band-Matched Catalog sources. The large H II complexes 30 Doradus, N11, N84, and N66 are marked with circles for reference. BMC sources are distributed throughout the entire S250 image but are most highly concentrated in star formation and high gas column density regions.

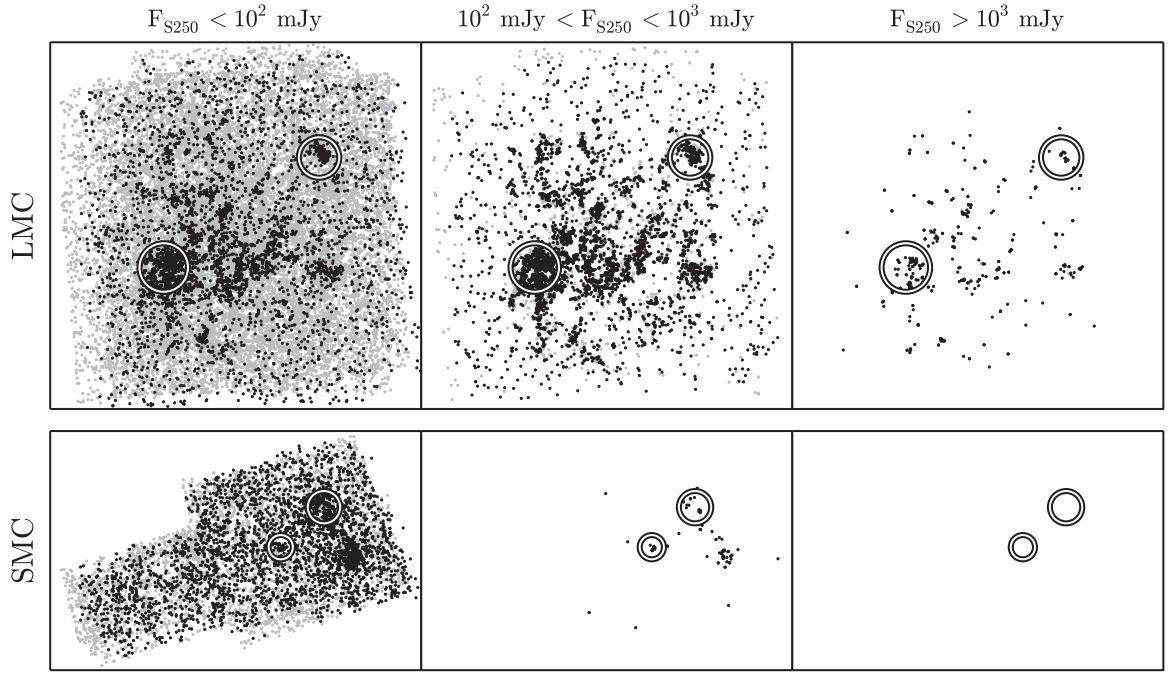

Figure 4. Positions of sources as a function of S250 flux for the LMC (top) and SMC (bottom). Sources detected in only SPIRE are marked in gray, while those with PACS detections (and possibly SPIRE as well) are marked with black. The positions of the prominent star formation regions from Figure 3 are marked with large circles to orient the reader.

(e.g., extreme and post-AGBs). We use a matching distance of 5″. If a BMC source is matched to multiple sources within a single literature catalog, the closest match is adopted. Likewise, if a previously classified source from the literature is matched to multiple BMC sources, only the closest match is kept. Below we document the catalogs to which we have matched, which is summarized in Table 6.

4.1.1. Young Stellar Objects

The first galaxy-wide search for YSOs in the LMC with *Spitzer* was conducted by Whitney et al. (2008), who photometrically identified ∼1000 candidate YSOs using the *Spitzer* SAGE data. An independent study by Gruendl & Chu (2009) also identified ∼1300 candidate YSOs in the LMC. Combined, the two studies identified ∼1800 unique YSO

Table 6
Literature Catalogs Matched to HERITAGE BMC

LMC		SMC	
Paper	Abbreviation	Paper	Abbreviation
YSOs			
Whitney et al. (2008)	W08	Bolatto et al. (2007)	B07
Gruendl Chu (2009)	GC09	Simon et al. (2007)	S07
Chen et al. (2009)	Chen09	Carlson et al. (2010)	Carlson10
Chen et al. (2010)	Chen10	Sewilo et al. (2013)	S13
Romita et al. (2010)	R10	Spectroscopically confirmed[a]	SpecYSO
Sewilo et al. (2010)	S10	Chen et al. (2014)	C14
Woods et al. (2011)	W11		
Carlson et al. (2012)	Carlson12		
Spectroscopically confirmed[a]	SpecYSO		
Background Galaxies			
Gruendl Chu (2009)	GC09	Kozlowski Kochanek (2009)	KK09
Kozlowski Kochanek (2009)	KK09	Veron-Cetty Veron (2010)	VV10
Gruendl Chu (2009)	GC09	Kozlowski et al. (2013)	K13
Veron-Cetty Veron (2010)	VV10	Sturm et al. (2013)	S13
Woods et al. (2011)	W11		
Kozlowski et al. (2013)	K13		
Evolved Stars			
Gruendl Chu (2008)	GC08	Boyer et al. (2011)	B11
Gruendl Chu (2009)	GC09		
Woods et al. (2011)	W11		
Boyer et al. (2010)	B10		
Boyer et al. (2011)	B11		
Van Aarle et al. (2011)	VA11		
Riebel et al. (2012)	R12		
PNs			
Reid Parker (2006)	RP06	G. Jacoby (2014, private communication)[b]	SMC-PNs
Gruendl Chu (2009)	GC09		
Hora et al. (2008)	H08		
Woods et al. (2011)	W11		
SNR			
Magellanic Cloud SNR database[c]	MCSNRD	Magellanic Cloud SNR database[c]	MCSNRD
Miscellaneous-dust Clumps, H II regions, normal stars, and unknown classifcation			
Gruendl Chu (2009)	GC09		
Woods et al. (2011)	W11		

[a] The catalog of spectroscopically confirmed YSOs were compiled by J. M. Oliveira (2014, private communication).
[b] The catalog of all known PNs in the SMC was complied by George Jacoby.
[c] The catalog of all known MC SNRs is maintained in the MCSNR Database operated by Rosa Williams and can be accessed online at http://www.mcsnr.org/about

candidates. YSOs can often be difficult to distinguish from other mid-IR bright sources such as background galaxies and evolved stars, and both studies quantified this difficulty by classifying the candidate YSOs into several categories. Whitney et al. (2008) distinguished "YSO candidates" from "high-probability YSO candidates," while Gruendl & Chu (2009) created three categories, which, listed from most to least certain, are "definite YSOs," "probable YSOs," and "possible YSOs." There are discrepancies between the two lists owing to their different source identification criteria, particularly for their least-confident classifications, but the lists agree reasonably well for those classified as "high-probability" or "definite" YSO candidates.

Because they were conducting galaxy-wide searches, Whitney et al. (2008) and Gruendl & Chu (2009) used relatively conservative brightness thresholds in order to remove the typically dimmer background galaxies from their YSO lists, thus selecting only the brightest, most massive YSOs. Smaller-scale studies of individual star formation regions can relax these criteria, because the investigators can do detailed

morphological inspections of each source. Such studies were conducted by Chen et al. (2009, 2010), Romita et al. (2010), and Carlson et al. (2012) of the large LMC H II complexes N11, N44, N51, N105, N113, N120, N144, N159, N160, and N206. Together, these studies identified an additional ~1000 YSO candidates in these LMC star formation regions.

Sewiło et al. (2013) conducted a detailed galaxy-wide photometric search for YSOs in the SMC by combining the techniques of Whitney et al. (2008) and Gruendl & Chu (2009) and identified ~1000 candidate YSOs. The sources are categorized into "possible YSO candidates" and "high-reliability YSO candidates." A previous study by Bolatto et al. (2007) identified candidate YSOs in a subregion of the SMC that includes only the main body of the galaxy, but their sources were not individually inspected as in Sewiło et al. (2013) and are potentially more contaminated by non-YSOs. Like in the LMC, several smaller-scale studies of SMC star formation regions identified additional, lower-luminosity YSOs: Chen et al. (2014), Simon et al. (2007), and Carlson & Meixner (2011) identified YSO candidates in the SMC Tail, N66, and N90, respectively.

A preliminary study of *Herschel*-detected LMC YSOs is presented by Sewiło et al. (2010) utilizing the HERITAGE observations. The survey selected sources by hand from a strip across the galaxy during the science demonstration phase of HERITAGE. In this strip of the LMC, which covered roughly $2° \times 8°$ of the LMC, 207 candidate YSOs were identified.

A number of mid-IR spectroscopic studies have confirmed the classification of MC objects as having YSO-like spectra, and a list of spectroscopic YSOs has been compiled by J. M. Oliveira (2014, private communication). Included in the compilation are targeted studies of MC YSOs by Oliveira et al. (2009, 2013), Shimonishi et al. (2008, 2010), van Loon et al. (2010a; 2010b), and Seale et al. (2009), who identified a number of mid-IR bright objects with YSO-like mid-IR spectra, most of them in the LMC. Woods et al. (2011) present the classification of 197 point sources observed with the Infrared Spectrograph on *Spitzer* in the SAGE-Spec Legacy program, 29 of which were categorized as YSOs. Woods et al. (2011) also identifies one object as an H II region, often considered a later stage of massive YSO evolution, as we do here. In total there are ~300 spectroscopically confirmed YSOs in the LMC, but only ~30 in the SMC.

4.1.2. Background Galaxies

One of the major contaminants in the *Spitzer* YSO surveys identified in Section 4.1.1 above are background galaxies, particularly at low flux levels. The nearest of these are spatially resolved in *Spitzer* images and can be distinguished from YSOs by their morphology. Indeed, during the process of identifying LMC YSOs, Gruendl & Chu (2009) identified probable non-YSO contaminants from their SEDs, location with respect to gas tracers, and morphology.

Using the SAGE LMC images and *Spitzer* images of the body of the SMC from the S^{3}MC survey (Bolatto et al. 2007), Kozłowski & Kochanek (2009) identified ~5000 candidate active galactic nuclei (AGNs) behind the MCs from their mid-IR photometry using color–magnitude diagrams (CMDs). As some galaxies occupy similar places in color–magnitude space as YSOs, unless they can be morphologically distinguished, there is expected cross-contamination between the AGN and YSO lists. Indeed, there is some overlap between sources identified as *candidate* galaxies by Kozłowski & Kochanek (2009) and as *candidate* YSOs in the YSO surveys discussed above. Known *confirmed* quasars were compiled by Veron-Cetty & Veron (2010), several hundred of which are behind the MC system, and a recent spectroscopic survey by Kozłowski et al. (2013) has confirmed the classification of 565 quasars behind the LMC and 193 behind the SMC. There are 87 AGNs identified behind the SMC by Sturm (2013) from their X-ray and radio emission. Finally, in their SAGE-Spec classification paper, Woods et al. (2011) identified a handful of potential galaxies.

4.1.3. Evolved Stars

Dust forms in the atmospheres of stars, and consequently, stars in late stages of evolution (extreme and post-AGBs) can emit in the FIR. Boyer et al. (2011) identified tens of thousands of evolved star candidates in the LMC and SMC from *Spitzer* images and photometrically classified them into several categories of evolved star including C-rich AGBs, O-rich AGBs, RSGs, and extreme AGBs. Of those, extreme AGBs are the most likely to be potentially FIR bright. Boyer et al. (2011) further identified populations of sources within each of these evolved star categories whose SEDs rise from 8 to 24 μm, which is typical of background galaxies, PNs, or YSOs. They reclassified these sources, which meet AGB and RGB color selection criteria, as "FIR objects." It is possible that a small number of extremely enshrouded evolved stars exist among these FIR objects, and so we include them in the evolved star category. We matched the BMC only to the extreme-AGB and FIR lists from Boyer et al. (2011).

Multiwavelength photometry was fit to a pre-computed evolved star model grid by Riebel et al. (2012) to classify LMC evolved stars selected by their IR colors and fluxes, and we adopt their list of stars best fit to extreme-AGB models. While Gruendl & Chu (2009) made mid-IR color–magnitude cuts to exclude the bulk of the AGB population, models suggest that there can exist some evolved stars embedded in a dusty envelope that will have colors similar to YSOs. Consequently, during the process of identifying YSOs, Gruendl & Chu (2009) documented ~100 red sources they suspected to be very red evolved stars. In their spectroscopic survey, Woods et al. (2011) identified nearly 150 evolved stars.

van Aarle et al. (2011) provides a catalog of 1407 candidate post-AGB stars in the LMC. They selected sources from the SAGE data with a 24 and 8.0 μm flux ratio F(24)/F(8) >0.4. YSOs, PNs, and background galaxies meet this same criteria, so substantial contamination from other source types, particularly YSOs, is expected.

We also include matches to two narrower studies. The *Herschel* FIR emission from three evolved massive stars in the LMC has been previously analyzed by Boyer et al. (2010). Gruendl et al. (2008) present a mid-IR spectroscopic study of 13 objects identified by their extremely red *Spitzer* colors, and confirmed them to be extreme carbon stars, documented here as extreme AGBs.

4.1.4. Planetary Nebulae

Reid & Parker (2006) compiled a list of all the known PN candidates in the LMC, which stood at 629 at the time of publication. Most of the PN candidates were identified from a combination of Hα images and the ratios of optical ionized gas

Table 7
BMC Classification Tables'[a] Contents

Column	Name	Description	Null
1	Source Name	The identifying name of the source.[b]	⋯
2	RA(J2000)	Right Ascension, J2000 (deg)	⋯
3	Decl.(J2000)	Declination, J2000 (deg)	⋯
4	ProbYSO	HERITAGE probable YSO candidates. 1 for yes, 0 for no.	⋯
5	PosYSO	HERITAGE possible YSO candidates. 1 for yes, 0 for no.	⋯
6	ProbDust	HERITAGE probable YSO candidates. 1 for yes, 0 for no.	⋯
7	PosDust	HERITAGE possible YSO candidates. 1 for yes, 0 for no.	⋯
8	HERGalaxy	HERITAGE background galaxy candidates. 1 for yes, 0 for no.	⋯
9	LitClass	Classification of positionally matched literature source[c,d]	⋯
10	LitRef	Reference for positionally matched literature source[c,e]	⋯
11	LitDist	Distance between BMC source and literature source[c] (arsec)	⋯
12	FarIRLum	Graybody-fit far-IR luminosity ($L_{\odot}$)	–999
13	FarIRLumUnc	Uncertainty of graybody-fit far-IR luminosity ($L_{\odot}$)	–999
14	FarIRTemp	Graybody-fit far-IR dust temperature (K)	–999
15	FarIRTempUnc	Uncertainty of graybody-fit FIR dust temperature (K)	–999

[a] Available from the *Herschel* Science Archive.
[b] A description of source name construction is found in the text.
[c] In the case of multiple matches, each match is separated by a "/."
[d] Source type abbreviations: YSO—young stellar object; posYSO—possible YSO; probYSO—probable YSO; defYSO—definite YSO; hpYSO—high probability YSO; hrYSO—high reliability YSO; Evol—evolved star; XAGB—extreme AGB; postAGB—post AGB; FIR—far-IR object; RSG—Red Supergiant; LBV—Luminous Blue Variable; WR—Wolf-Rayet star; Gal—background galaxy; posGal—possible background galaxy; PN—planetary nebula; SNR—supernova remnant; D—dust clump; S—normal star; Unk—unknown.
[e] Literature reference abbreviations are given in Table 6.

emission lines. However, some contamination of this PN list by compact H II regions powered by O/B stars is expected, and hence a YSO or regular star classification would be more appropriate (Reid & Parker 2010). A list of known PNs in the SMC was compiled by G. Jacoby (2014, private communication) presented the mid-IR photometry of LMC PNs identified in the SAGE data, and as with previous categories of sources, Woods et al. (2011) spectroscopically identified 7 PNs, and Gruendl & Chu (2009) identified ∼50 PN candidates in the SAGE data.

4.1.5. Supernova Remnants

At the time of writing this paper, there is no unified catalog of all known SNRs in the MCs in the literature, although a catalog of all confirmed SNRs in the MCs is maintained online in the Magellanic Cloud Supernova Remnant Database[21] by the Magellanic Cloud Supernova Remnant Collaboration (Murphy Williams et al. 2010). Most of the remnants are ∼20 pc to over 100 pc in diameter, large enough to be resolved in the *Herschel* observations and thus would not be included in the HERITAGE point source catalogs. However, the youngest remnants are compact and unresolved. Indeed, the youngest remnant in the LMC, that of SN 1987 A, is a point source in the HERITAGE data, and was previously analyzed in Matsuura et al. (2011).

4.1.6. Miscellaneous

Several additional miscellaneous types of sources may be present in the HERITAGE catalogs. In particular, normal stars located near a dust cloud can heat the dust sufficiently to be detected in the IR. Similarly, diffuse clumps of dust can be warmed by the ISRF and may be detected as a point source in the FIR. Gruendl & Chu (2009) and Woods et al. (2011) identified sources of these types from their *Spitzer* photometry or spectroscopy, and classified them as either normal stars or diffuse dust clumps. Finally, IR-bright sources that could not be classified by Woods et al. (2011) were assigned the "unknown" classification.

[21] http://www.mcsnr.org/

Table 8
Statistics of Matches to Previously Known Sources

Number of Matches		Number Matched to Other Type				
	Total	YSOs	Galaxies	Evolved Stars	PNs	SNR
			LMC			
YSOs	1298	⋯	309	261	26	0
Galaxies	1126	309	⋯	110	7	0
Evolved stars	443	261	110	⋯	17	0
PNs	45	26	7	17	⋯	0
SNR	2	0	0	0	0	⋯
			SMC			
YSOs	624	⋯	59	34	7	0
Galaxies	152	59	⋯	6	4	0
Evolved stars	51	34	6	…	2	0
PNs	9	7	4	2	⋯	0
SNR	0	0	0	0	0	⋯

4.2. Matching to Previously Classified Sources: Results

Along with the BMCs, the *Herschel Science Archive* hosts two additional tables (one for each galaxy) that identify matches to the above listed literature catalogs of previously classified LMC and SMC objects. Table 7 documents the columns of these tables, while Table 8 collates some statistics of the matching. A total of 2272/733 BMC sources in the LMC/SMC were found to have literature matches. We find the

highest number of matches to YSOs, with 1298 and 624 BMC sources being coincident with previously identified YSOs in the LMC and SMC, respectively. We also find a large number of matches to sources previously identified as being background galaxies—1126 in the LMC and 152 in the SMC. There are far fewer for the SMC because the Kozłowski & Kochanek (2009), Kozłowski et al. (2013), and Veron-Cetty & Veron (2010) galaxy searches were restricted to only the main bar of the SMC, a significantly smaller area than the LMC.

Between the two galaxies, we find ∼500 matches to sources previously identified as candidate evolved stars: 299 post-AGBs, 51 extreme AGBs, 186 FIR objects from Boyer et al. (2011), and 11 candidate evolved stars from Woods et al. (2011) or Gruendl & Chu (2009). These sources are discussed in more detail in later sections, but most of them have likely either been improperly identified as evolved stars in the literature or are mismatches with the BMC. In addition, we find a small number of PNs (54), SNRs (2), dust clumps (48), and normal stars (58). Note that the classifications are not mutually exclusive, as classifications can differ by author. In particular, we find significant overlap between sources classified as YSOs and background galaxies—of the 1298/624 sources identified as candiate YSOs in the LMC/SMC, 309/59 of them have been classified as potential background galaxies in a separate paper. We highlight one particularly extraordinary example: source HSOBMHERICC J79.075912-71.899396. We identified three different previous classifications in the literature by Gruendl & Chu (2009), Whitney et al. (2008), and Kozłowski & Kochanek (2009), who classified it as an evolved star, a high-probability YSO, and a background galaxy, respectively. This source was also later observed spectroscopically by Woods et al. (2011), who could not match it to a known spectral type and put it in the "unknown" category. This source highlights the difficulty in classifying dusty objects that photometrically look similar in the IR. The biggest overlaps exist between YSOs and background galaxies, YSOs and evolved stars (primarily post-AGBs and FIR objects), and YSOs and PNs.

4.3. Identifying New Background Galaxy Candidates

One of the major constituents of the HERITAGE point source catalogs are background galaxies. As discussed above, over 1200 BMC sources are coincident with previously identified background galaxies. The *Herschel* Key Project Astrophysical Terahertz Large Area Survey (ATLAS; Eales et al. 2010), an extragalactic survey that has mapped large sections of the sky at 100, 160, 250, 350, and 500 μm, detected thousands of galaxies (nearly 7000 in the ∼16 square degree *Herschel* Science Demonstration Phase data) with S250 fluxes that ranged between ∼10 and 10^3 mJy and an inverse power-law flux distribution. Extrapolating to the sky area and applying the sensitivity of HERITAGE, there are potentially several thousand background galaxies in the HERITAGE images and significantly more than were matched to previously identified galaxies in the literature.

We have separated those sources most likely to be background galaxies from those residing in the MCs by analyzing the flux distribution and FWHM of the sources in the HERITAGE images. Many HERITAGE sources appear slightly extended beyond the PSF, however background galaxies should be distant enough to be point-like in the SPIRE images. The vast majority of sources located in the MCs are dust clumps and YSOs, which at these wavelengths are not observed to be perfectly point-like sources, but rather compact density peaks contained within larger structures whose density falls with distance from the source.

We define point-like sources as those whose S250 FWHM reported in the HERITAGE Catalog agrees within 10% of the PSF FWHM in Table 1. In cases where no S250 point source was identified or the S250 FWHM could not be measured (due to the background being too complex or the source too faint), a source is deemed point-like if either of the other SPIRE sources' FWHMs agrees within 10% with the corresponding PSF. A small number of sources are not detected in any SPIRE bands, in which case we apply the same criteria to the PACS detections. In Figure 5, we show the positions of all BMC sources in the MCs. The left-hand panels show sources with a measured FWHM consistent within 10% with the adopted PSF FWHM (Meixner et al. 2013), while the right-hand panels show sources larger than the PSF. Sources that are extended are concentrated on the body of the MCs and in recognizable Galactic structures, while those with FWHMs similar to that of the PSF reside over the entire image, including in the outer regions of the MCs, the expected behavior if background galaxies tend to be point-like and YSOs/dust clumps are not.

There are 12,142 point-like sources in the LMC and 5333 in the SMC, not all of which are necessarily background galaxies, as evolved stars or compact, isolated YSOs may also appear to be point-like. Below we compare the flux distribution of these sources to that expected from background galaxies.

4.3.1. Background Galaxy Flux Distribution

To estimate the number of the point-like sources expected to be background galaxies, we obtained the ATLAS Science Demonstration Phase source catalogs, which covered an approximately 4° × 4° area of the sky (Rigby et al. 2011), and contains the *Herschel* fluxes for 6876 galaxies. The ATLAS team used the S250 image to identify galaxies; compared to the PACS images, their SPIRE data has lower noise such that any source detected by PACS would also be detected by SPIRE. This mirrors the sensitivity of our observations, where both the poorer sensitivity of and low-level striping in PACS data has resulted in a brighter PACS completeness limit relative to SPIRE. Due to the galaxies' inverse power-law flux distribution their numbers are dominated by the faintest sources, and as a consequence, most of the background galaxies in the HERITAGE images have fluxes near the sensitivity limit of our observations. The ATLAS observations are deeper than that of HERITAGE, so the faintest galaxies detected in the ATLAS survey would not be identified in our images. Thus, predicting the number of background galaxies in HERITAGE requires the application of the HERITAGE catalog's completeness.

Recall from Section 3.1 that the completeness of the HERITAGE catalogs—and thus the number of detected background galaxies—is dependent on the level of background emission from the ISM where the sources are located. At low background surface brightness, $B_{\nu,S250} \leqslant 10$ MJy sr^{-1}, the completeness is well-defined; Figure 25 in Meixner et al. (2013) shows the S250 catalogs to be 100% complete above 100 mJy, with a completeness that quickly drops to 0% at 20 mJy. Quantifying the completeness at high backgrounds is less secure, because it is highly sensitive to the brightness and structural complexity of the background emission. Meixner

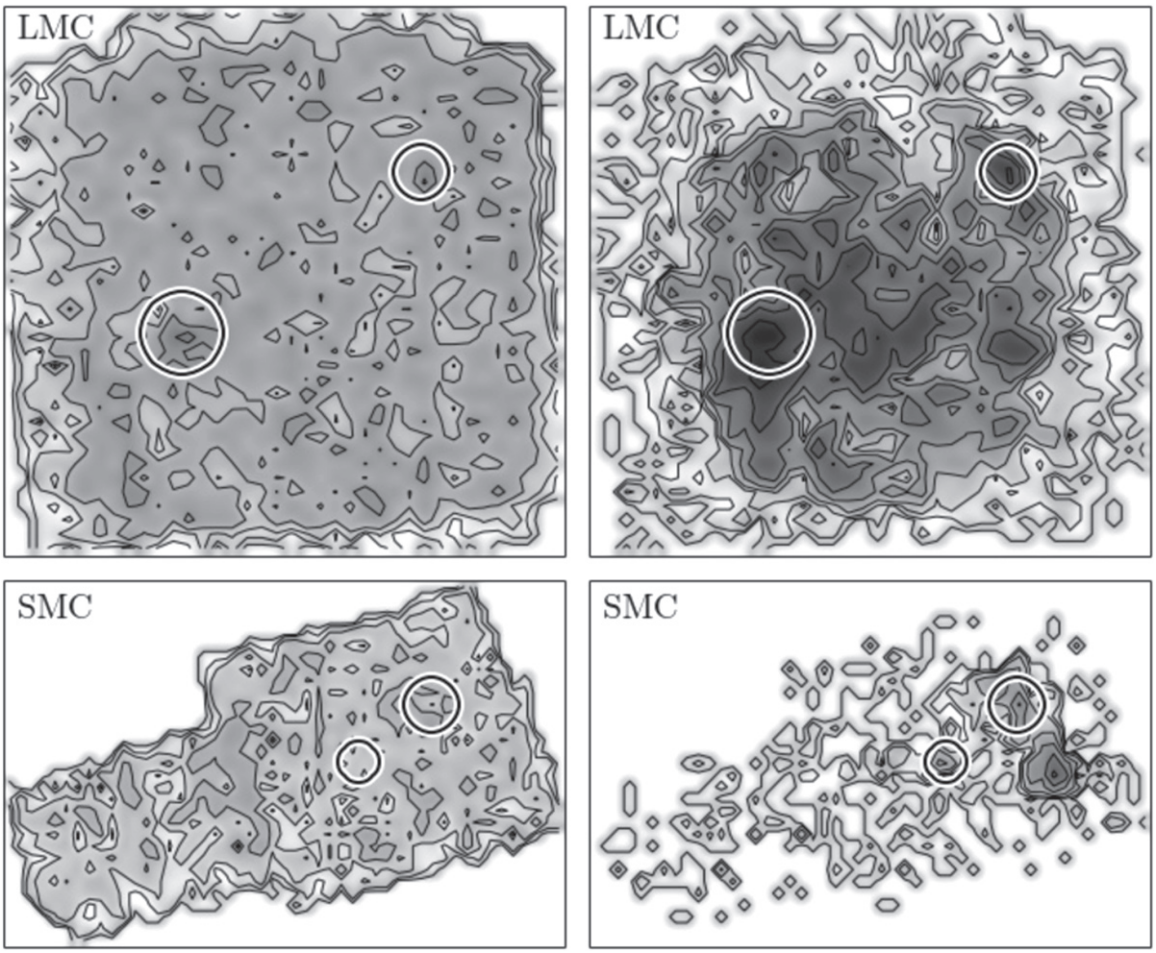

Figure 5. Surface number density of S250 sources in the LMC (top) and SMC (bottom). The left-hand panels show sources with a FWHM within 10% of the PSF's FWHM, while the right-hand panels show those that are more than 10% larger than the PSF. Contour levels are drawn at source densities of 25×2^n kpc^{-2} ($n = 0,\ 1,\ 2,\ 3$ ...). The locations of the prominent star formation regions from Figure 3 are marked with large circles.

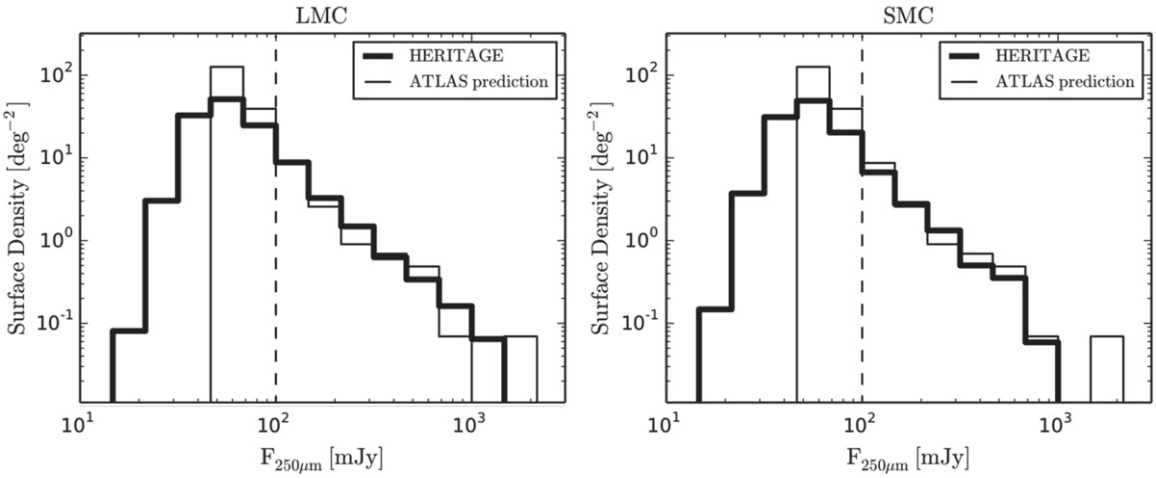

Figure 6. Flux distribution of galaxy candidates in low background from HERITAGE (thick line) compared to the prediction from ATLAS (thin line) for HERITAGE after applying the HERITAGE full list completeness curve to the raw distribution. The two curves agree very well above ~100 mJy, where a vertical dashed line marks the HERITAGE S250 100% completeness limit.

et al. (2013) presents a sample completeness curve for sources located within a characteristic high background region in the LMC ($B_{\nu,\mathrm{S250}} > 10$ MJy sr^{-1}); the typical S250 completeness for that particular region is 100% above 1 Jy, ~60% at 100 mJy, and 0% below 20 mJy. However, this completeness curve cannot be applied to all high background regions, where the surface brightness varies by more than two orders of magnitude. We are thus best able to predict the number of detected background galaxies in low-background regions, while in high-background regions we can only set upper limits.

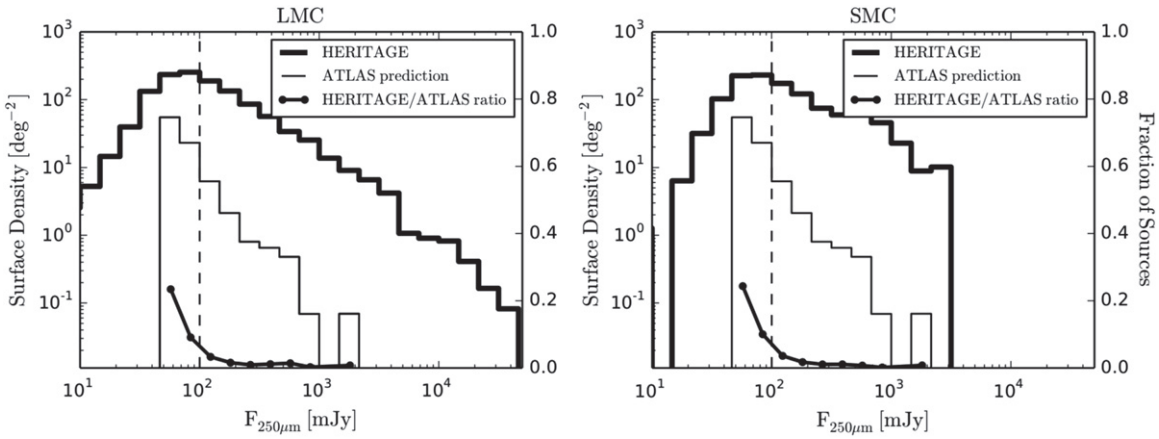

Figure 7. Same as Figure 6, but for sources located in high backgrounds. The number of HERITAGE sources greatly outnumbers the number of predicted background galaxies. The black lines with points are associated with the right axes, and show the ratio of the number of galaxies predicted by ATLAS and the number of HERITAGE point sources.

Recall that the low background areas account for the majority of the HERITAGE images, however the natural correlation between MC-residing sources and ISM means that many faint sources will be confused with the ISM and be undetected.

Figure 6 shows a comparison between the flux distribution (shown as a source surface number density) between ATLAS and HERITAGE. The thick-lined histogram shows the flux distribution for point-like HERITAGE sources in a low background ($B_{\nu,S250} \leqslant 10$ MJy sr^{-1}). When available, we adopt the background surface brightness provided in the HERITAGE catalogs; when not, it is measured off the background image (a "source-less" S250 image modeled by StarFinder during source extraction) as the mean value in a 6×6 pixel box centered at the position of the source. Sources located off the S250 image are assumed to be in low background. The thin-lined histograms show the surface number density of galaxies from the ATLAS survey after applying the HERITAGE full list completeness curve. Above 100 mJy (where both surveys are complete), the two curves are in good agreement. Recall that the HERITAGE S250 catalog is only complete above 100 mJy, explaining the divergence of the HERITAGE flux distribution and the ATLAS prediction below 100 mJy. Given the point-like nature of these HERITAGE sources, their good agreement with the expected flux distribution predicted by ATLAS, and their positional distribution in the outer regions of the MCs, we classify point-like objects in a low background as "HERITAGE galaxy candidates." There are 10,558 galaxy candidates in the LMC HERITAGE image and 5410 in the SMC's.

The comparison with ATLAS is less straightforward in high background regions where the completeness is highly variable. Figure 7 shows the flux distribution of all HERITAGE sources in high background ($B_{\nu,S250} > 10$ MJy sr^{-1}) with the thick-lined histogram. Similar to Figure 6, the thin-lined histogram is the predicted galaxy flux distribution after applying the characteristic high background HERITAGE full list completeness curve from Meixner et al. (2013) to the raw ATLAS distribution. Note that there are significantly more HERITAGE sources than can be accounted for by background galaxies. The black curve with points, the values of which are marked on the right-hand axis, shows the ratio of the HERITAGE and predicted galaxy histograms at fluxes above 50 mJy, where ATLAS is complete. The curve shows a very low fraction of galaxies at high flux levels, and an increasing fraction with decreasing flux. Above 100 mJy, there are 6841/460 HERITAGE sources in the LMC/SMC, but ATLAS predicts only 127/8 (<2%) to be galaxies. Clearly the vast majority of sources in high background regions are MC-residing sources, and we therefore do not classify any sources in high backgrounds as galaxy candidates. However, from the predicted flux distribution, we estimate that in high background regions, ~10% of sources brighter than 50 mJy, <2% brighter the 100 mJy, and none brighter than ~1 Jy are in fact background galaxies.

4.3.2. Comparison to Previously Identified Galaxies

Of the 798 BMC sources coincident with previously identified galaxies in a low background, 710 (89%) of them were recovered in the above procedure and were classified as galaxy candidates. Those that were not have an average measured FWHM that is 1.2 times larger than the PSF, slightly too large to be identified as point-like, and were thus rejected as candidate galaxies. Approximately 1/3 of them are resolved in *Spitzer* observations to be background spiral galaxies oriented face-on with respect to the sky, such that their relatively large angular size prevented their identification as candidate galaxies from the HERITAGE data. Some contamination of the HERITAGE galaxy candidate list is expected from point-like MC sources located in low backgrounds such as evolved stars and isolated YSOs. Of the 9745/5,111 galaxy candidates identified in the LMC/SMC, 217/190 (2%/4%) were previously identified as non-galaxies; however 104/8 of those 217/190 were also identified as galaxies by alternate investigators. We therefore estimate possible non-galaxy contamination of the HERITAGE candidate galaxy list at 1–2% in the LMC and <4% in the SMC. Contamination of the galaxy candidate list by non-galaxies in the SMC is potentially higher because of the SMC's lower dust content, which makes MC-residing sources dimmer and less extended at *Herschel* wavelengths, and thus more likely to be identified as point-like.

In summary, we have identified 10,558 and 5410 galaxy candidates in the HERITAGE LMC and SMC images, respectively, in low background regions, in good agreement with the number predicted by a comparison with the ATLAS survey. The number of galaxies in high background regions is difficult to assess given the variable background/completeness.

However, the number of sources expected to be background galaxies in high background regions decreases with increasing flux; no galaxies are expected to be brighter than 1–2 Jy.

4.4. Identifying New YSO, Young Cluster, and Dust Clump Candidates

4.4.1. Young Stellar Objects

YSOs warm the dust in their circumstellar environment, making them bright in the IR and among the largest populations of objects in the HERITAGE catalogs. At the earliest stages of formation, when YSOs are enshrouded in significant gas and dust, photospheric and accretion emission is reprocessed by the circumstellar envelope, and YSOs' SEDs peak in the FIR (Evans 1999). In fact, the youngest, most embedded sources are dominated by their FIR emission and may show little to none in the mid- or near-IR. The SED evolves as the forming star dissipates its surroundings (Whitney et al. 2003), revealing mid-IR emission originating from warmer dust nearer the star. By the latest stages of formation, the circumstellar envelope is dissipated, and the SED is dominated by emission from the stellar photosphere (UV, optical, and near-IR) and possibly a circumstellar disk (near- and mid-IR). The HERITAGE survey is thus most sensitive to the early and middle stages of star formation, when the YSOs are embedded within the circumstellar material from which they are forming.

Indeed, in Section 4.1 we identified sources coincident with previously known YSOs primarily identified in the mid-IR with *Spitzer*, and find that 1298/624 BMC sources from the LMC/SMC are coincident with YSOs identified by mid-IR photometry. The vast majority of these previously identified YSOs (95%) have a coincident 24 μm source from the SAGE and SAGE-SMC point source catalogs that are incorporated into the BMC. Inspection of the small percentage of sources without a 24 μm counterpart shows that in all cases there is mid-IR emission at the position of the source, but that the emission was not identified in the 24 μm SAGE/SAGE-SMC catalogs due to the source being saturated or extended, and thus not identified as a point source during automated source extraction.

The lists of previously identified YSOs in the literature are incomplete, particularly those that surveyed the entirety of the MCs. In part, the incompleteness results from the necessity when doing large surveys to set conservative color and magnitude cuts that eliminate significant contamination from non-YSO populations such as evolved stars and background galaxies. YSOs can arguably be better separated from evolved stars in the FIR, where bright emission from an evolved star is rare; only $\sim$1% of the BMC sources are coincident with a previously identified evolved star, and most of those were classified as YSOs in other studies. A significant fraction of the BMC is background galaxies, but Section 4.3 demonstrated that these can be reliably identified—in low background regions—from their point-like nature, and make up only a small fraction of sources in high backgrounds. Therefore, the HERITAGE data is well-suited to identify YSOs that were missed by the *Spitzer* investigations.

We have identified sources in the BMC that are most likely to be YSOs by making a series of cuts to the BMC. We describe the cuts below, and refer to them as Cuts 1–3.

Cut 1: We first consider only sources that are detected in at least three *Herschel* bands, which eliminates a large number of very faint sources that are identified in only one or two images. While there are likely true YSOs among those eliminated, it is difficult to accurately characterize a source with little photometric data. We consider also only sources that are either not in a group (recall Section 2.2), are the "dominant" source in a group, or are in a group and brighter than 200 mJy (the S250 catalog 100% completeness limit for the >99% of the image with a background of <100 MJy sr^{-1}) in at least one of the unblended PACS bands. This ensures that that we only consider sources whose measured photometry is—at least in part—the result of its own emission and not a nearby source or group member.

Cut 2: We next eliminate sources previously identified in the literature as non-YSOs and those we identified as being background galaxy candidates; we do not eliminate sources that were also previously identified in the literature as YSOs. This procedure recovers 1017/435 (78%/70%) of the BMC's previously identified YSOs in the LMC/SMC. Those not recovered were on the faint end of the flux distribution and were thus not bright enough to be detected in at least three *Herschel* bands in Cut 1. The SMC's lower dust content makes YSOs fainter than in the LMC, and thus a larger fraction do not meet the three-band detection requirement.

Cut 3: Not all of these sources are necessarily YSOs; at the faintest flux levels, there can be contamination from background galaxies, and some sources may be starless, externally illuminated dust clumps, which could look like point-like, FIR sources in the MCs (see below). Unlike starless dust clumps, middle- to later-stage YSOs will have bright 24 μm point-like emission from the YSOs' warm/hot circumstellar dust. For this reason, the presence of 24 μm emission is a common tracer for star formation activity (see review by Dunham et al. 2014, and references therein). We therefore classify as YSO candidates sources for which we have identified a coincident 24 μm source from SAGE/SAGE-SMC. As discussed in Section 4.3, background galaxies make up a small fraction (<2%) of HERITAGE sources with a S250 flux greater than 100 mJy, but a larger fraction at lower fluxes. We therefore classify sources with S250 fluxes $\geqslant$100 mJy as "probable YSO candidates," and those dimmer as "possible YSO candidates."

Following Cut 3, there are 2493 probable YSO candidates and 1025 possible YSO candidates in the LMC, and there are 425 probable and 238 possible YSO candidates in the SMC. Approximately 67% of these are newly identified YSO candidates in the LMC, 24% in the SMC.

4.4.2. Dust Clumps

Sources that pass Cuts 1 and 2 but fail Cut 3 are likely dusty, MC-residing sources, but their lack of a coincident 24 μm point source in the SAGE/SAGE-SMC catalogs prevents them from being identified as candidate YSOs. We classify these objects as "candidate dust clumps." Like with YSOs, there is potential confusion with background galaxies, thus we distinguish between "probable" ($F_{S250} \geqslant 100$ mJy) and "possible" ($F_{S250} < 100$ mJy) dust clumps. We use the term dust clump very generally, simply referring to the fact that they have the photometric properties of a compact, dusty source located within the MCs. There are 1175/1569 probable/possible dust clump candidates in the LMC and 36/74 in the SMC. These sources are most likely a combination of starless clumps, forming clusters, and YSOs.

Photometrically, all of these source types can look very similar in the FIR. A YSO's FIR emission originates from the dusty material surrounding the forming star that absorbs and reprocesses the radiation from the internal, embedded source.

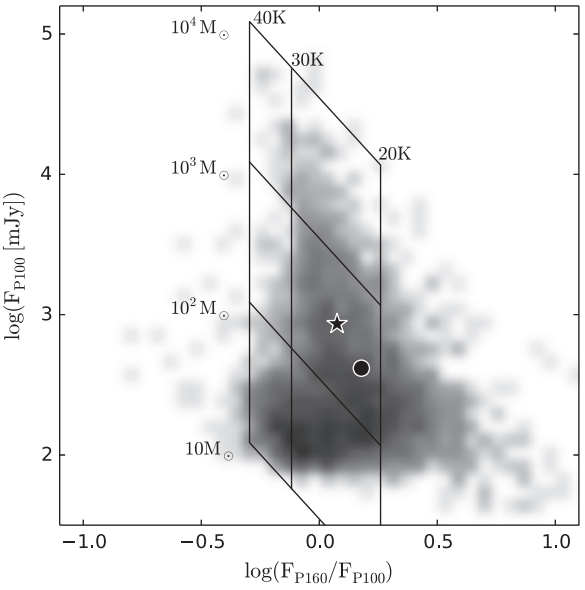

Figure 8. PACS F_{160} and F_{100} CMD. BMC sources are shown as a Hess diagram. Lines indicate the region of CMD space occupied by graybodies with indicated gas masses and dust temperatures. The star and dot mark the locations of the modeled YSO and starless clump described in the text.

But such a dusty clump can also be warmed by an *external* illuminator such as a nearby star or the ISRF. If the dust clump is sufficiently point-like, then these starless clumps can be difficult to distinguish photometrically from clumps harboring a deeply embedded forming star. In Figure 8 we compare the PACS photometry of the HERITAGE sources to graybody curves for optically thin clumps with dust temperatures of 20–40 K and total gas masses of 10–10^4 $M_\odot$. We adopt a dust opacity that scales with frequency as $\kappa_\nu = f_{\rm dust} \times 0.1 \times (\nu/10^{12}\ {\rm Hz})^\beta\ {\rm cm^2\ g^{-1}}$ (Beckwith et al. 1990), where $\beta = 1.5$, $f_{\rm dust} = 0.5$ is the dust abundance relative to solar for the LMC, and opacity is measured per gram of gas (e.g., Galliano et al. 2011).

Figure 8 also shows the location in CMD space of two dust clumps modeled with a three-dimensional radiative transfer model (Whitney et al. 2013)—one contains an embedded 2×10^3 $L_\odot$ protostar, while the other is starless and is illuminated by an ISRF 10 times the ISRF in the solar neighborhood (ISRF$_\odot$; Mathis et al. 1983; Chandrasekhar 1960). Note that both clumps have similar FIR fluxes and dust temperatures of between 20 and 30 K despite their different sources of illuminating radiation. In principle, the measured FIR flux of all sources results from a combination of warming from any embedded source and the ISRF. If the luminosity of the central source greatly exceeds the luminosity the clump absorbs from the ISRF, then the ISRF warming is negligible. Conversely, if the embedded star's luminosity is sufficiently low, the warming of the dust clump is dominated by the ISRF.

We estimated the typical luminosity absorbed from the ISRF by a MC clump by modeling a starless clump and integrating its SED to determine its luminosity. We modeled a clump with a radius of 1.5×10^5 AU, approximately 0.75 pc, typical of dense clumps resolved with millimeter observations in the LMC (Seale et al. 2012). Such a source would be point-like in *Herschel* observations at the MC distance. The typical ISRF in the MCs varies between 1 and 10 times the solar neighborhood value, but can reach strengths as high as 20–100 times on the inside edges of large PDRs surrounding OB associations (e.g., Bernard et al. 2008; Galametz et al. 2013). In order to define a maximum *typical* luminosity for starless clumps, we adopt a value of 10 × ISRF$_\odot$. Integrating the resulting SED gives a maximum starless clump luminosity of ∼1000 $L_\odot$. If a clump is brighter than this value, then it is either located within a high ISRF not typical of most of the MCs, or it contains an embedded source whose luminosity exceeds 1000 $L_\odot$.

Figure 9 shows the FIR luminosity distribution of sources we have classified as probable/possible YSOs and dust clumps. Section 5.1 below describes how we determine the luminosity of BMC sources. Note that in both cases, the S250 flux cut separating the "probable" and "possible" source classification skews the "probable" sources to higher luminosities than their "possible" counterparts. Dust clumps brighter than 1000 $L_\odot$ are more luminous than can be explained by a typical ISRF, implying the existence of an embedded source. In fact, while the dust clumps do not have a matching 24 μm SAGE/SAGE-SMC point source, many of them have mid-IR emission at the position of the source identifiable in the *Spitzer* images. This emission was not identified as a SAGE/SAGE-SMC point source, because it is not sufficiently point-like; it is either extended or saturated. This is true of all of the very high luminosity ($L_{\rm far\text{-}IR} > 10^5$ $L_\odot$) dust clumps, where the sources are so bright at 24 μm they saturated the detector. These high-luminosity dust clumps are truly high-mass YSOs. Dust clumps with luminosities of <1000 $L_\odot$ are dim enough that their luminosity can be explained solely by the re-radiation of the ISRF. While these clumps must not contain any high-mass YSOs, they are *not* necessarily starless.

Visual inspection of the dust clumps in *Spitzer* images reveals some of them to be resolved into several or many clustered sources at *Spitzer* resolution, again preventing their identification as a point source at 24 μm. Such a morphology is typical of small, forming clusters that still contain their natal gas and dust that is radiating in the FIR. BMC sources that *Spitzer* reveals to have a cluster-like morphology may be YSOs or young clusters.

5. DISCUSSION

5.1. Far-Infrared Luminosity Distribution

The integrated FIR luminosity is estimated for a subsample of the BMC for which there was ample photometry to perform a reliable reduced χ^2 fitting of the *Herschel* photometry to a graybody curve. Graybody fits to sources detected in only one band are completely unconstrained, and fits to only two photometry points are unreliable. We therefore only fit sources that are detected to better than 3σ in at least three *Herschel* bands; this eliminates a large number of very faint sources. We also only fit sources that are either not in a group or are the "dominant" source in their group, ensuring that the photometry being fit is primarily the result of its own emission. Using the graybody model described in Section 4.4.2 and used in Figure 8, we fit all sources that meet these criteria and then scale the integrated flux to the distance of the MCs to determine the FIR luminosity, which is reported in the classification tables along with the fit dust temperatures, which have typical values of 10–30 K.

The *Herschel* photometry reported in Meixner et al. (2013) and used here contains a four-flag system for grading the

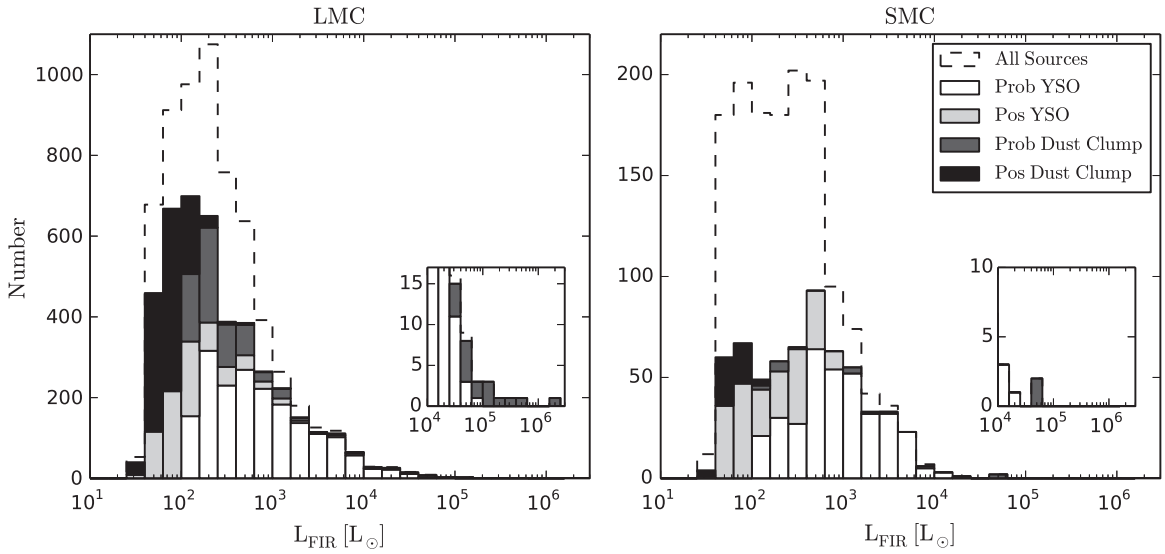

Figure 9. Far-IR luminosity distribution of the subsample of the LMC's BMC for which the luminosity could be estimated from a graybody fit. All sources are shown with the black curve, while YSOs and dust clumps are shown in the colored histograms. The inserts show a zoom-in on the sources with luminosities $>10^4$ $L_\odot$. YSOs are generally brighter than dust clumps, and probable YSOs/dust clumps are brighter than their possible YSO/dust clump counterparts.

quality of the photometric extraction. Fluxes with a flux flag of 1 are of highest quality, and we perform the fit using the reported measurements and uncertainties (σ). A flux flag of 2 is a less-secure measurement, and thus we increase the uncertainties to 2σ. In some instances, fluxes with a flux flag of 3 may be better-treated as upper limits, so we increase the upper uncertainty bound to 3σ and leave the lower uncertainty at 1σ. Flux flag 4 sources have highly uncertain fluxes, and we perform the fit with 3σ uncertainties. We find sources to range in luminosity from several tens of $L_\odot$ to $\sim 10^6$ $L_\odot$, and Figure 9 shows the FIR luminosity distribution for all LMC sources fit.

Figure 9 further breaks down the luminosity distribution into YSO and dust clump candidates. Probable YSOs have FIR luminosities between $\sim 10^2$ and $\sim 10^5$ $L_\odot$, with an average value of $\sim 1.5 \times 10^3$ $L_\odot$. Possible YSO candidates necessarily have a lower S250 flux, and their average FIR luminosity of ~ 200 $L_\odot$ is correspondingly lower. Probable dust clumps range in luminosity between $\sim 10^2$ and $\sim 10^5$ $L_\odot$, with an average of $\sim 5 \times 10^3$ $L_\odot$, higher than that of probable YSOs. The average luminosity of the probable dust clumps is dominated by the few sources with luminosities $>10^4$ $L_\odot$ seen in the inset figures. These high luminosity dust clumps are almost certainly YSOs that have not been classified as such because they saturated the *Spitzer* detector at 24 μm. Possible dust clumps have a much lower average luminosity of ~ 60 $L_\odot$.

The vast majority of the non-YSO sources with a fit FIR luminosity have been classified as background galaxies; a small fraction are evolved stars, PNs, and SNRs. For sources located outside the MCs, the FIR luminosity is an unphysical quantity.

5.2. Mid-Infrared Photometry

We use the BMC to inspect the mid-IR photometry of FIR sources. In Figures 10 and 11, we present [8.0] versus [8.0]–[24] CMDs for different classes of sources. In all panels, the size of the dot is proportional to the distance between the *Herschel* and *Spitzer* source; matches with a larger distance should be treated with more caution, as a mismatch between the catalogs may have occurred.

The lines in the figures are those from Sewiło et al. (2013) and Carlson et al. (2012) used to differentiate regions in CMD space occupied by different populations of sources. The bluer area left of the dashed curve contains primarily normal and evolved stars, while the redder region to the right contains YSOs and background galaxies. Evolved stars redden as they age and will cross the classification lines into the red region at later stages. At the distance of the MCs, the brightest YSOs will be brighter than the brightest background galaxies, so the black curve was introduced by Sewiło et al. (2013) to separate the brightest, most probable YSOs above the curve from the dimmer background galaxies below the curve. Note, however, that the separation between YSOs and galaxies is not sharp and that both YSOs and galaxies can occupy the space to the right of the dashed curve.

The top rows of the figures show BMC sources matched to previously classified objects. Previously identified YSOs and background galaxies are located on the red side of the diagram, with galaxies tending to have dimmer mid-IR magnitudes, consistent with the CMD classification lines. The brightest previously identified galaxies have also been identified as YSOs in other studies, as indicated by the black-outlined circles.

BMC sources previously identified as evolved stars occupy a wide range of CMD space. Many of the evolved star candidates to the right of the classification curves have also been previously identified as YSOs. This is particularly true for the post-AGB candidates, and most of these sources are likely incorrectly classified as evolved stars. We demonstrate this below in Section 5.5. Moreover, many previously identified evolved stars have a large matching distance to the HERITAGE source, as indicated by the large size of the dot in the CMDs. This is expected for dim sources such as the FIR objects and some of the post-AGB candidates, as their lower flux leads to higher positional uncertainties. But this is not expected for very bright sources such as the extreme AGBs with [8.0] of approximately 8 dex. The HERITAGE sources matched to the extreme carbon stars with large matching distances are almost

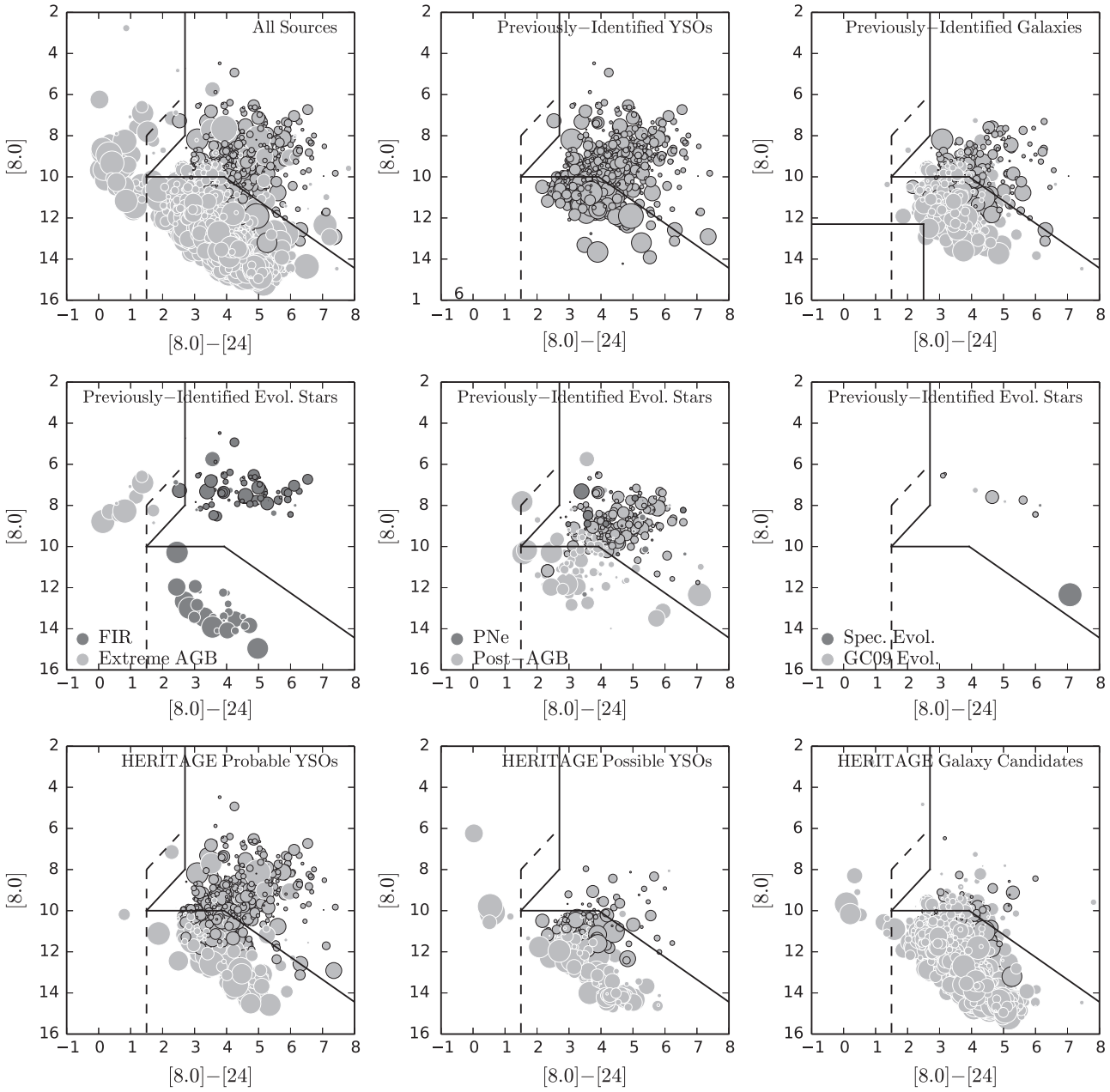

Figure 10. [8.0] vs. [8.0]–[24] CMD for the BMC sources in the LMC. Zero-point fluxes are taken from the IRAC and MIPS handbooks. Each panel shows a different population of sources as indicated at the top of the panel. The center panels show various evolved stellar types, which are differentiated by the shade of the marker's face as indicated in the bottom of the panel. Note that classifications are not mutually exclusive. Sources of different types tend to occupy different regions of CMD space, but heavy overlap exists, resulting in multiple, differing classifications for some sources. In particular there is a high number of sources that have been classified as non-YSOs (both here and in the literature) that have also been classified as YSOs by other authors. In all panels, sources previously classified as YSOs are indicated with a black outline around the point. The dotted and solid lines show the YSO classification cuts defined in Carlson et al. (2012) and Sewiło et al. (2013), respectively.

certainly mismatches and therefore a misclassification of the BMC source as an evolved star.

5.3. Spatial Distribution

Figures 12 (LMC) and 13 (SMC) show the positions of the BMC sources of different classification throughout the MCs. The evolved stars appear to be concentrated toward the center of the LMC and the main body of the SMC, the expected distribution if they mimic the stellar distribution. By contrast, the distribution of background galaxies in the LMC is consistent with a homogeneous population of distant sources uncorrelated spatially with MC structures. Our HERITAGE galaxy candidate identification procedure (Section 4.3) restricted the identification of *new* background galaxies to regions of low background, so some of the anti-correlation between galaxies and MC structures is built into the process. In the SMC, the majority of the previously identified galaxies come from the study by Kozłowski & Kochanek (2009), who only searched directly behind the main body of the SMC and the Wing. Therefore the distribution of previously identified galaxies in the SMC is not representative of the true distribution.

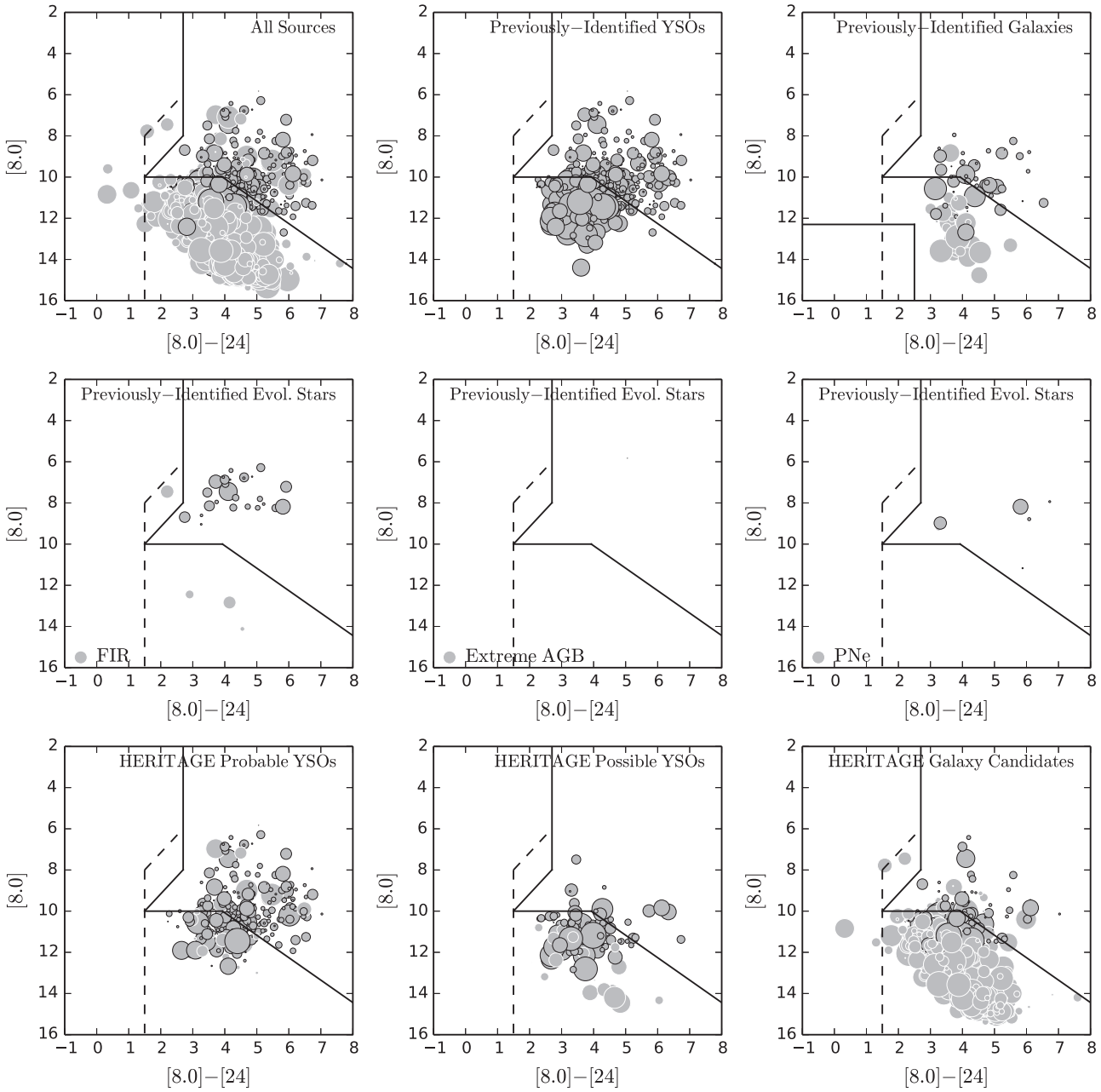

Figure 11. Same as Figure 10, but for the SMC and with some evolved star panels moved as indicated in the legend. Only one extreme AGB (which was also previously identified as a YSO) has ample IRAC photometry to be plotted; it is represented in the figure by a very small dot due to its small matching distance.

The panels showing the distribution of YSOs demonstrate a completely different distribution. YSOs tend to be concentrated around molecular clouds or the many large H II complexes seen in Hα emission (e.g., 30 Doradus; Figure 3), meaning the YSOs are correlated with regions of dense gas and active, massive star formation. The dust clumps have a similar distribution, consistent with their being dusty knots of material in regions with significant ISM. The higher radiation field in H II complexes provides a logical source of external illumination for the clumps.

5.4. Herschel-Detected Young Stellar Objects: Characteristics and Completeness

The two largest prior searches for LMC YSOs by Whitney et al. (2008) and Gruendl & Chu (2009) identified 1385 and 958 YSO candidates, respectively, for a total of ∼1800 unique sources. The corresponding study in the SMC by Sewiło et al. (2013) identified 1024. Of these, 888 are here classified as HERITAGE YSO candidates in the LMC and 402 in the SMC. A larger fraction of previously identified YSOs are detected by *Herschel* in the LMC than the SMC likely due to the LMC's higher dust content, such that otherwise identical YSOs with the same stellar and circumstellar gas mass will be brighter in the LMC than the SMC.

The HERITAGE BMCs contain 2559 LMC and 234 SMC HERITAGE YSO candidates (probable plus possible) that were previously unidentified in the literature, greatly increasing the number of suspected MC YSOs, particularly in the LMC. The newly identified YSOs are in general fainter than those known prior to this study. Figure 14 shows the BMC sources'

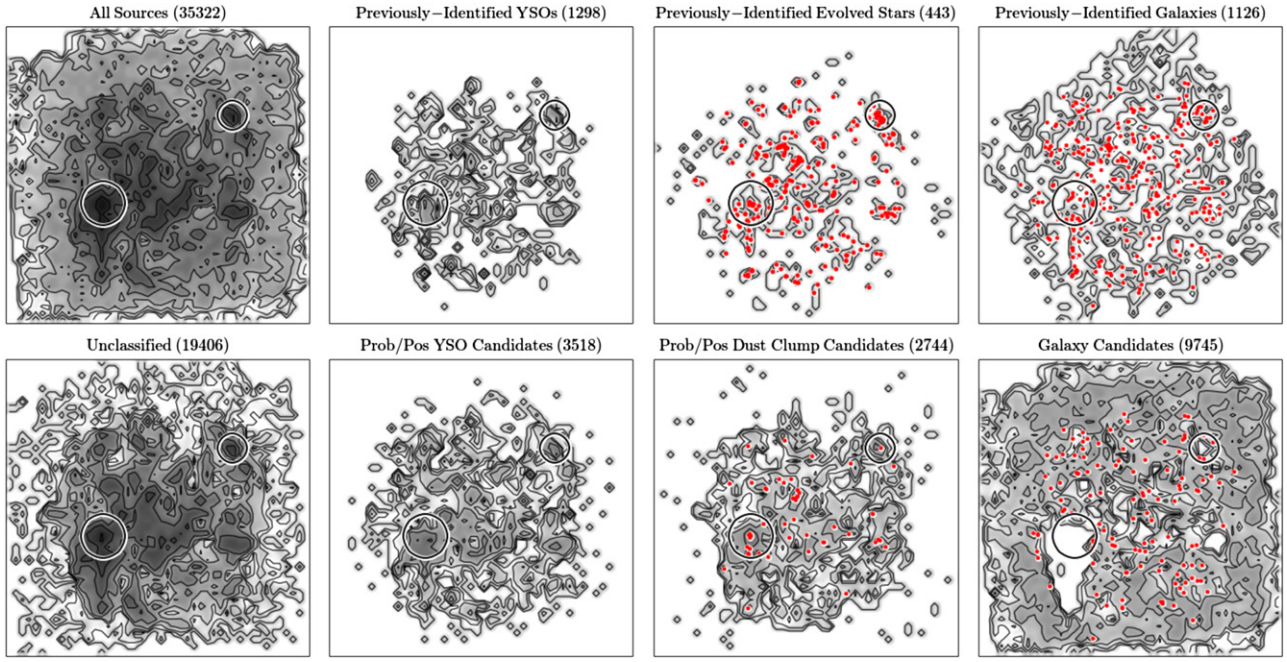

Figure 12. Number surface density for BMC sources in the LMC. All sources are shown in the upper left panel, while the other panels show the indicated populations. In the right and right-center panels, sources also previously identified as YSOs are marked with red dots. In all panels, the number in parentheses next to the population name indicates the number of sources in that population. Contour levels are drawn at source densities of 25×2^n kpc^{-2} ($n = 0,\ 1,\ 2,\ 3\ldots$).
(A color version of this figure is available in the online journal.)

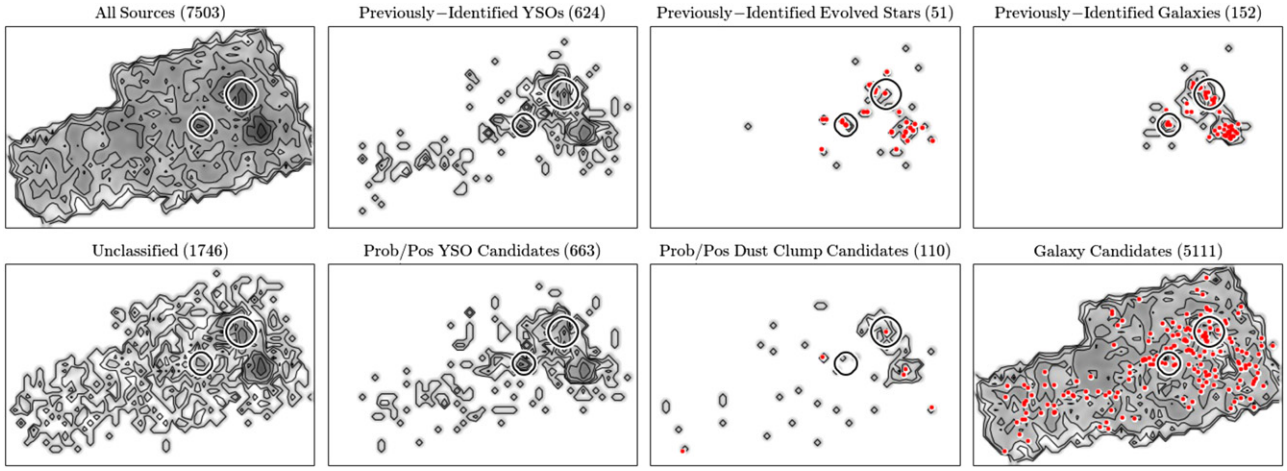

Figure 13. Same as Figure 12, but for the SMC.
(A color version of this figure is available in the online journal.)

estimated FIR luminosity as a function of their S250 flux. The two variables are not independent, so correlation is built into the process. Note that previously identified YSOs tend to be located on the high luminosity end of the correlation, and that the newly identified YSO candidates extend to fainter luminosities. Cut 1 in the YSO candidate selection criteria biases toward brighter sources. Adopting the catalog completeness limits quoted in Section 3.1, we estimate the HERITAGE candidate YSO lists to be complete above a flux of 400 mJy in any *Herschel* band, which corresponds to the flux above which 100% of BMC sources pass Cut 1. If we make a best-fit line to the luminosity–flux correlation seen in Figure 14, this flux limit roughly corresponds to a luminosity completeness limit of 1000 $L_\odot$, which is the luminosity of a $\sim$6 $M_\odot$ main-sequence star (spectral type B4; Cox 2000). Note that this completeness limit applies only to the population of YSOs *Herschel* is sensitive to, i.e., embedded FIR bright YSOs. Later-stage, less embedded YSOs will not be detected. Indeed, many previously identified YSOs are not detected by HERITAGE.

Figure 15 shows the IR SEDs of a sample of LMC YSO candidates that combine *Spitzer* and *Herschel* photometry. The SEDs rise from the mid-IR to the FIR, typical of early to mid-stage YSOs. The FIR peak indicates the presence of a circumstellar envelope that reprocesses stellar and accretion radiation and emits it in the FIR. The new YSO candidates, particularly the probable candidates, closely mimic the SEDs of the previously identified sources. The less-luminous possible YSO candidates tend to be detected in fewer *Herschel* and

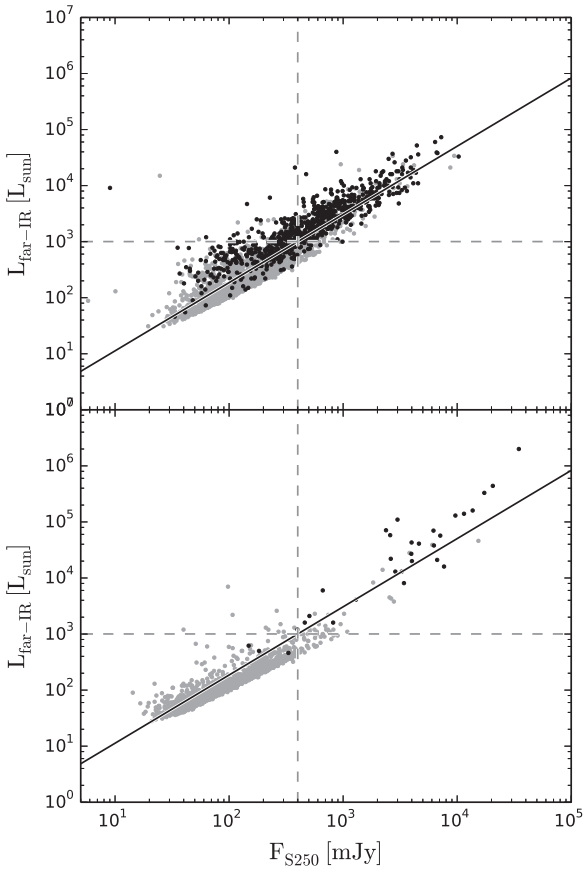

Figure 14. Far-IR luminosity of HERITAGE LMC YSOs (top panel) and dust clumps (bottom panel) as a function of S250 flux. Sources previously identified as YSOs are shown in black, while the rest are in gray. The solid black line shows the best fit to the correlation considering both populations, $\log_{10}\left(L_{\text{Far-IR}}\ [L_{\odot}]\right) = 1.2 \times \log_{10}\left(F_{S250}\ [\text{mJy}]\right) - 0.16$. The vertical dashed line shows the estimated 100% flux completeness limit for HERITAGE YSO candidates, and the horizontal dashed line marks the corresponding luminosity limit given the best fit line, $\sim$1000 $L_{\odot}$.

Spitzer bands (many are detected only in the more sensitive SPIRE images), and so the shape of the FIR peak is poorly defined. The dotted curves in Figure 15 show the best fit graybodies when there is ample photometry to perform the fit from which the FIR luminosity is derived. As previously identified YSO candidates (numbered 1–7 in Figure 15) tend to be of higher luminosity, their *Herschel* fluxes are correspondingly high and the graybody fits are of better quality. This is in contrast to the possible YSO candidates (sources 15–21) whose *Herschel* fluxes are measured to less significance, resulting in poorer fits.

Figure 16 shows the SEDs of both previously identified background galaxies and newly classified HERITAGE galaxy candidates. The similarity between the shape of YSO and galaxy SEDs demonstrates the difficulty in using IR colors alone to differentiate the two populations. At low flux levels, the populations can look photometrically identical. In general, the previously identified galaxies represent the brightest objects of their type behind the MCs, and the high sensitivity HERITAGE images allow for the identification of fainter objects. Most are too dim to have been detected in the *Spitzer* images (e.g., sources 10, 11, 15, and 16 in Figure 16) and are seen in only 1–3 *Herschel* images (sources 15–17).

5.5. Herschel-Detected Evolved Stars

In Figure 17, we recreate the mid-IR CMDs from Figures 10 and 11 and show the SEDs of a sample of the post-AGB candidates from van Aarle et al. (2011). The shaded region in the CMD is the color selection criteria used by van Aarle et al. (2011) to select candidate post-AGB stars. The shaded region heavily overlaps with the regions used in YSO studies recreated from Figures 10 and 11, thus explaining the high number of sources previously identified as both post-AGB and YSO candidates. Indeed, the post-AGB SEDs resemble those of YSOs. Five of the BMC post-AGB candidates were observed with low resolution optical spectra presented in van Aarle et al. (2011) in order to confirm their classification as post-AGBs. The positions of these five sources in CMD space are marked in the left-hand panel and their SEDs are shown in the center panel. BMC sources HSOBMHERICC J73.375205-69.296953 (source 1 in the figure), HSOBMHERICC J78.854807-66.317713 (2), HSOBMHERICC J80.919272-68.090965 (3), and HSOBMHERICC J83.220747-69.987453 (5) were all confirmed to have post-AGB like spectra and classified as Of/Of?, Ae, B3Iep, and G5 stellar types, respectively. HSOBMHERICC J82.644586-68.104609 (source 4) was of unknown type and marked "?" in van Aarle et al. (2011); we classify it as a HERITAGE galaxy candidate, and our own inspection of the source in *Spitzer* images reveals it to have an edge-on disk morphology, indicating it is unequivocally a background galaxy and not a post-AGB star.

One can estimate the total dust mass that must be present to account for the estimated FIR luminosity by using the dust temperature from the graybody fits and using a dust opacity, $\kappa = 4.1\,\text{cm}^2\,\text{g}^{-1} \times (\lambda/100\,\mu\text{m})^{-1.5}$ (Sodroski et al. 1987). Theoretical models predict AGB stars to produce total dust masses on the order of 10^{-4} to 10^{-2} $M_{\odot}$ per star (Ferrarotti & Gail 2006; Zhukovska & Henning 2013). HSOBMHERICC J82.644586-68.104609 (source 4 in Figure 17) is a background galaxy so the fit is unphysical; the fit to source HSOBMHERICC J78.854807-66.317713 (2) is too poor to accurately determine the mass, and HSOBMHERICC J80.919272-68.090965 (3) lacks ample photometry to fit. The fits to sources HSOBMHERICC J73.375205-69.296953 (1) and HSOBMHERICC J83.220747-69.987453 (5) imply a total dust mass on the order of $\sim 10^{-2}$ $M_{\odot}$, which is on the high end of the expected AGB dust production range. However, *most* of the photometrically identified post-AGB candidates have fit dust masses that *greatly* exceed reasonable AGB star dust production. The mean total fit dust mass for the photometrically identified post-AGB candidates is 1.5 $M_{\odot}$; all 210 non-spectroscopic post-AGB candidates have a fit dust mass of $>3 \times 10^{-2}$ $M_{\odot}$, and $\sim$90% have a dust mass $>10^{-1}$ $M_{\odot}$. In fact, the dust mass implied for some of these post-AGB candidates unphysically exceeds the mass of AGB progenitors. However, these dust masses are typical for the parsec-scale clumps of gas that harbor massive YSOs and forming clusters. The conclusion is that while some of the BMC post-AGB candidates (including the spectroscopic post-AGBs, except for HSOBMHERICC J82.644586-68.104609) may be evolved stars, the benefit of *Herschel* photometry leads us to conclude most of them are actually YSOs. Note, however, that this applies only to those detected by *Herschel* and not the entire catalog of $\sim$1400 post-AGB candidates presented in van Aarle et al. (2011).

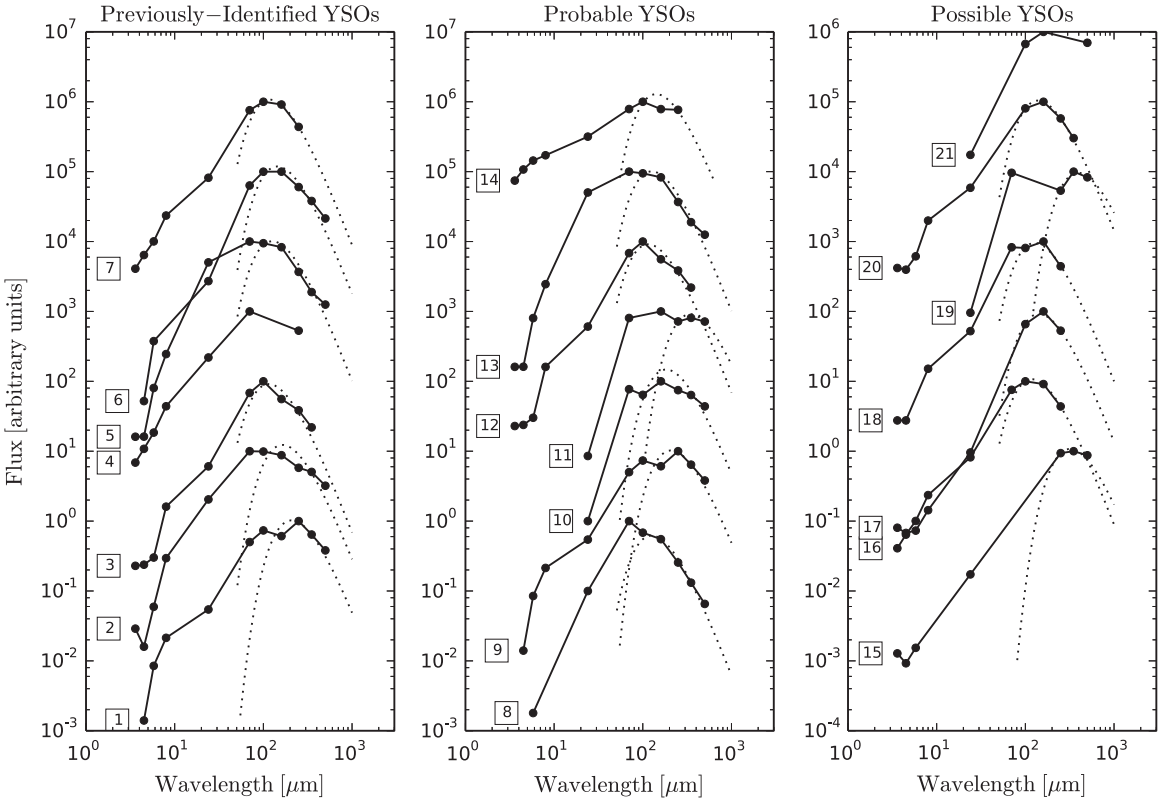

Figure 15. Sample of SEDs of previously identified YSOs (left), probable YSO candidates (center), and possible YSO candidates (right) combining *Spitzer* and *Herschel* photometry. Sources are numbered for easy reference in the text.

There are 44 LMC and 7 SMC BMC sources matched to extreme AGB star candidates. A sample of their SEDs is shown in Figure 18. As discussed above, most of these are likely mismatches; there are only 17 in the LMC and 4 in the SMC if we consider only sources within 1″ of the matched literature source, and a vast majority of those (14 in the LMC and 3 in the SMC) have also been classified as YSOs in alternate studies. The likelihood of mismatch is supported by the discontinuities seen in their SEDs; examples include sources 12 and 13 in Figure 18. However, some sources are likely good matches (e.g., sources 14 and 15), and one can test the feasibility of their being extreme AGBs by repeating the dust mass analysis we did for post-AGB candidates. In the LMC, all 8 of the sources for which there is ample photometry have an estimated dust mass $>0.5\ M_{\odot}$; these sources are not extreme AGBs. In the SMC, HSOBMHERICC J13.483718-70.634514 has a fit dust mass of $\sim 2 \times 10^{-2}\ M_{\odot}$, a high, but reasonable total dust production mass for an AGB. However, HSOBMHERICC J21.033974-73.15116 contains nearly $1\ M_{\odot}$ of dust, and is not an AGB. Two LMC BMC sources, HSOBMHERICC J82.683128-71.716888 and HSOBMHERICC J87.249164-70.556065, have been confirmed with mid-IR *Spitzer* spectroscopy to be extreme carbon-rich AGB stars (Gruendl et al. 2008). The SEDs of these two sources, marked 10 and 11, are shown in Figure 18, and the smooth transition between *Spitzer* and *Herschel* photometry implies the BMC is associated with these confirmed extreme AGBs. In summary, of the 44/7 LMC/SMC BMC sources matched to previously identified extreme AGBs, about half are likely mismatches between the BMC and the AGB candidate. Of those with close matches, approximately half are too faint to estimate the dust mass, while nearly all the rest have dust masses too large to be extreme AGBs. Consistent with their alternate literature classification as YSOs, most of the BMC matches to extreme AGB candidates are probably actually YSOs. However, two spectroscopically confirmed extreme AGBs are in the LMC BMC, and one SMC BMC source has a fit dust mass comparable to that expected from AGB stars, and cannot be ruled out as an extreme AGB star.

Sources 8 and 9 in Figure 18 are two examples of the 186 AGB candidate "FIR sources." As suggested in Boyer et al. (2011), the original paper in which the FIR sources are classified, the FIR source SEDs are consistent with being background galaxies, YSOs, or PNs, and are likely not evolved stars. Moreover, they have a median fit dust mass of $\sim 1.5\ M_{\odot}$, inconsistent with AGBs.

SEDs of several PNs are labeled 3–6 in Figure 18. PNs have SEDs similar to YSOs and galaxies, rising from the mid-IR and peaking in the FIR. Indeed, of the 45/9 matches to LMC/SMC PNs in the literature, 26/7 have also been identified as YSOs, all of which have high ($>0.1\ M_{\odot}$) fit dust masses. The two SNRs, labeled 1 and 2 in Figure 18, are SNR J052501-693842 (also known as LHa-N132 D) and SN 1987 A, identified as HSOBMHERICC J81.264647-69.642784 and HSOBMHERICC J83.866283-69.269995, respectively, in the BMC. A careful analysis of the *Herschel* emission from SN 1987 A is presented in Matsuura et al. (2011), who found a total dust mass of 0.4–0.7 $M_{\odot}$, consistent within the error bars with the value obtained from our graybody fit of 0.3–1.1 $M_{\odot}$. Only detected in two *Herschel* bands, the emission from SNR J052501-693842 is too faint to accurately constrain the dust mass. The BMC source HSOBMHERICC J79.075912-

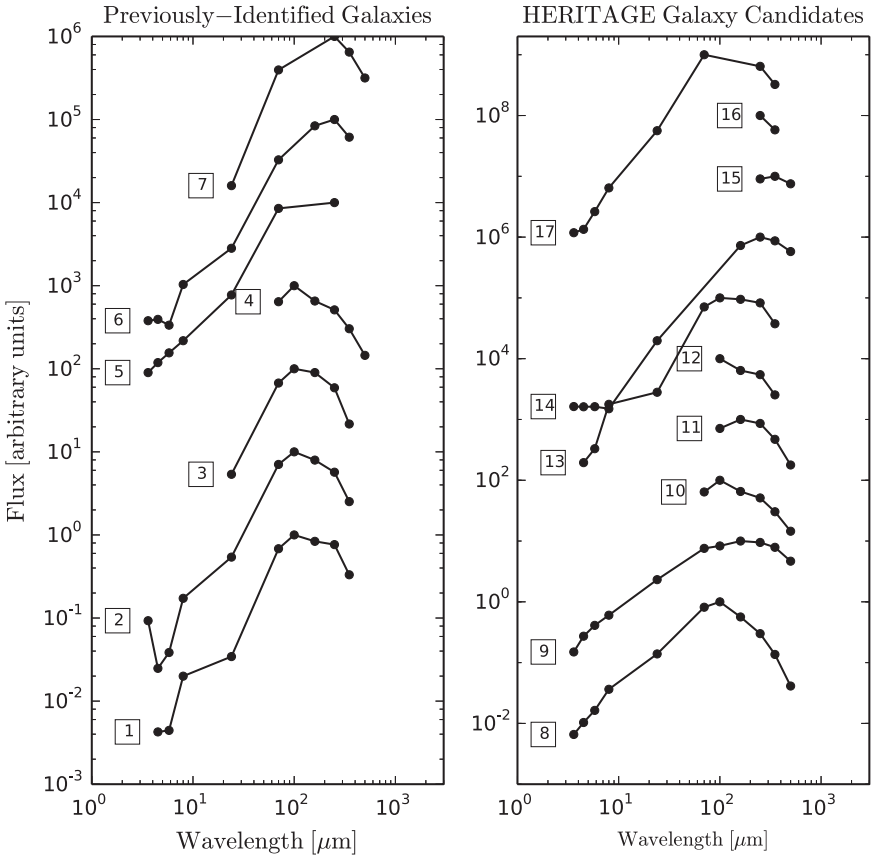

Figure 16. Same as Figure 15, but for previously identified galaxies (left) and new HERITAGE galaxy candidates (right).

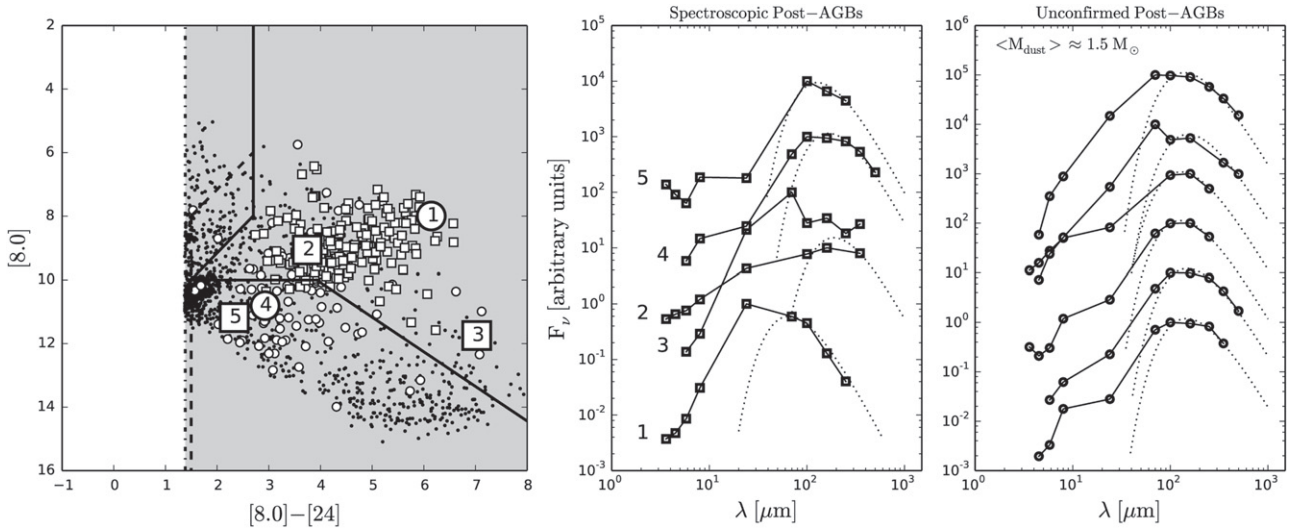

Figure 17. Left: [8.0] vs. [8.0]–[24] CMD. All post-AGB candidates from van Aarle et al. (2011) are shown with black dots, and those matched to a BMC source are marked with larger white symbols. Those also identified as YSOs in other studies are marked with white squares, while those that are not are marked with white circles. The positions of the five spectroscopic post-AGB candidates are marked with large numbered symbols. The shaded area denotes the region of CMD space used in van Aarle et al. (2011) to identify post-AGBs. The dashed and solid lines are the YSO classification cuts from Figures 10 and 11. Note that the post-AGB and YSO regions heavily overlap. Center: IR SEDs of the spectroscopic post-AGB candidates from van Aarle et al. (2011), numbered as is the left-hand panel. The dotted line shows the best-fit graybody curve for sources with ample quality photometry. Right: same as the center panel, but for a sample of the post-AGB candidates for which optical spectra were not taken in van Aarle et al. (2011).

71.899396 is the source of unknown spectral type from Woods et al. (2011). Its SED is consistent with a YSO, background galaxy, or PN, and it has a fit dust mass of $\sim$1 $M_{\odot}$, ruling out the possibility of it being an evolved star with a low-mass progenitor.

5.6. *Herschel*-Detected Dust Clumps

To have been classified as dust clumps, BMC sources must meet the following criteria: (1) pass Cuts 1 and 2 from Section 4.4.1, and (2) not have a coincident 24 μm source from the SAGE/SAGE-SMC catalogs. The first criterion excludes

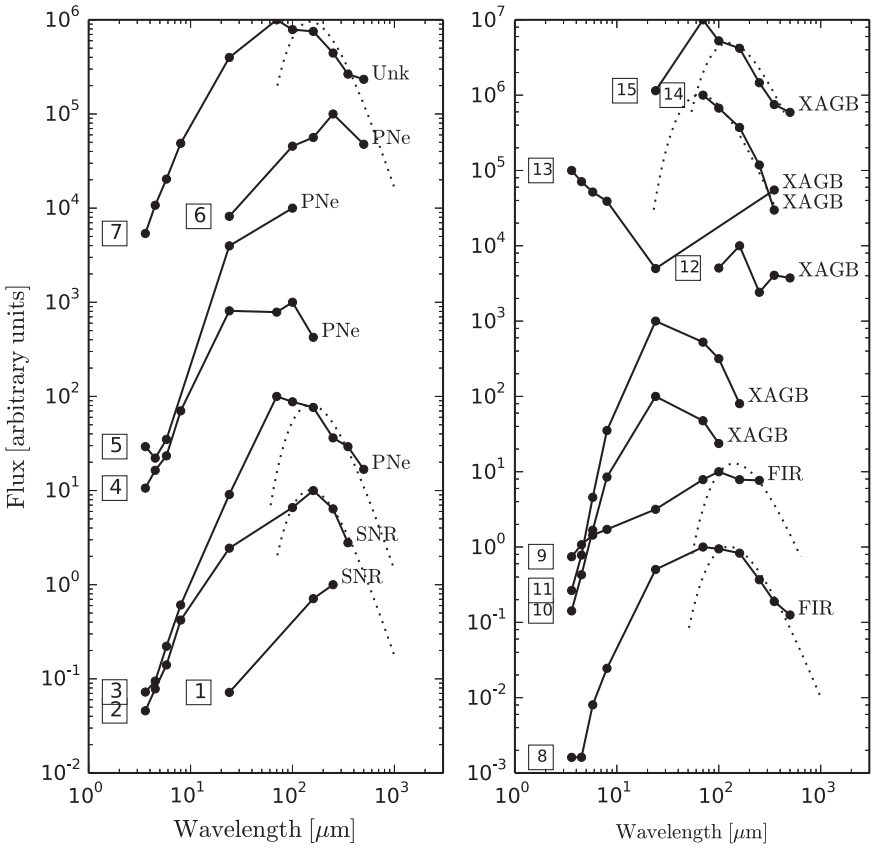

Figure 18. A sample of SEDs for BMC sources matched to stars in late stages of stellar evolution from the literature. PNs, SNRs, extreme AGBs, and far-IR objects are marked "PN", "SNR," "XAGB," and "FIR," respectively. One source of unknown spectral type from Woods et al. (2011) is marked "Unk." When there is ample photometry to perform a fit, the graybody of best fit is drawn with a dotted line. Sources are numbered 1–15 so as to be easily referenced in the text.

the faintest sources from the BMC that were only detected in 1–2 *Herschel* bands, while the second criterion separates the YSO candidates from those we classify as dust clumps. Indeed, Figure 14 demonstrates that the vast majority of sources previously identified as YSOs have a coincident 24 μm source and are therefore classified as HERITAGE YSO candidates. Note, however, the small number of HERITAGE dust clumps —particularly at high luminosity—that were previously identified as YSOs in the literature. As described above, these several dozen sources are almost certainly massive YSOs that saturated the MIPS detector and thus do not have a 24 μm counterpart in the SAGE/SAGE-SMC catalogs. Indeed, recall that sources with a FIR luminosity above $\sim$1000 $L_{\odot}$ are too bright to owe their entire luminosity to re-radiated interstellar radiation.

By contrast, HERITAGE dust clumps with FIR luminosities below $\sim$1000 $L_{\odot}$ show no sign of embedded star formation, and are thus classified as dust clumps. While their luminosities are consistent with being warmed by the ISRF and we detect no signs of star formation, we cannot determine without higher resolution and sensitivity imaging if these clumps are truly starless. The luminosity of embedded low-mass stars would be greatly overwhelmed by that of the ISRF, and their mid-IR flux may be below the SAGE/SAGE-SMC catalog detection limits. Nevertheless, the dust clumps are the best candidates for starless clumps in the MCs, and some of them may be the precursors to future star- and cluster-forming clumps. Indeed, recall that their spatial distribution mimics that of YSOs.

5.7. Unclassified BMC Sources

Of the 35,322/7503 BMC sources in the LMC/SMC, we identify a most likely classification for 15,916/5,757 of them by either matching them to catalogs in the literature or independently assigning a classification as YSO, dust clump, or background galaxy. That means approximately half of the BMC sources are left unclassified in the LMC and about one quarter are unclassified in the SMC. Those without classifications represent the dimmest sources in the BMC; too little of or too poor *Herschel* photometry was collected to analyze the photometric properties of the sources to acceptable accuracy. We can, however, inspect the spatial distribution of these sources and speculate as to their nature. The $\sim$19,000 unclassified LMC sources are distributed across the entire LMC, but are notably more concentrated in star formation regions and areas with high gas column densities (Figures 3, 12). The suggestion is that most of the unclassified LMC BMC sources are very faint YSOs, dust clumps, or ISM fluctuations that are too dim to pass Cut 1. Their distribution, however, is more distributed than that of the YSOs or dust clumps, and a great number of sources also lay on the outskirts of the galaxy, and are likely very dim background galaxies that are too faint for us to assess their point-like nature. The 1746 unclassified SMC sources have a similar positional behavior, but with a larger fraction of sources appearing to be background galaxies. This would be expected, as the SMC's lower dust content makes dust clumps and ISM fluctuations fainter.

Table 9
Statistics of HERITAGE Classifications

Number of Sources		Number Matched to Other Type in Literature				
	Total	YSOs	Galaxies	Evolved Stars	PNs	SNR
			LMC			
Galaxy Candidates	9745	118	679	118	3	0
Probable YSO Candidates	2493	824	182	199	21	0
Possible YSO Candidates	1025	135	53	12	1	0
Probable Dust Clump Candidates	1175	51	0	12	1	0
Possible Dust Clump Candidates	1569	7	0	2	0	0
			SMC			
Galaxy Candidates	5111	179	31	19	1	0
Probable YSO Candidates	425	319	34	25	4	0
Possible YSO Candidates	238	110	6	2	1	0
Probable Dust Clump Candidates	36	6	0	2	1	0
Possible Dust Clump Candidates	74	0	0	0	0	0

6. SUMMARY

We present band-merged point source catalogs for the MCs that combine the photometry from the *Herschel* HERITAGE and *Spitzer* SAGE surveys, which we call the HERITAGE BMC. We identify 35,322 and 7,503 unique FIR emitting objects in the LMC and SMC, respectively. The BMCs, which contain source positions, fluxes, flux uncertainties, and other photometric quantities are available from the *Herschel* Science Archive.

We positionally matched the BMCs to lists of potentially FIR bright objects in the literature including previously identified YSOs, background galaxies, PNs, SNRs, some types of evolved stars, normal stars, and dust clumps. Table 8 documents the lists from the literature to which we match. A total of 2272/733 BMC sources in the LMC/SMC were found to have literature matches. Tables hosted by the *Herschel* Science Archive report the results of the matching, which are summarized in Table 6. The primary results of the matching are as follows.

1. We find the highest number of matches to YSOs and background galaxies. In total, nearly 2000 BMC sources are matched to previously identified YSOs and ∼1300 to previously identified background galaxies. A larger fraction of the previously known YSOs in the LMC are identified in *Herschel* images relative to the SMC, presumably because of the LMC's higher dust content.
2. There are 443 matches in the LMC and 51 in the SMC to evolved star candidates that include extreme AGBs, post-AGBs, and FIR objects from Boyer et al. (2011). Post-AGB candidates account for the majority (299) of the evolved star matches. These candidate post-AGBs were color selected from their *Spitzer* colors (van Aarle et al. 2011) and are highly contaminated by YSOs. Indeed, ∼2/3 of the post AGB candidates are coincident with previously identified YSO candidates and have fit dust masses that greatly exceed that reasonably produced by AGB stars. Likewise, approximately half of the FIR sources are also candiate YSOs and have similarly high dust masses. We find atypically large matching distances between the BMC sources and previously identified extreme AGBs, suggesting possible mismatches between the catalogs. However, and least two extreme AGBs and four post-AGBs have spectroscopically confirmed classifications, and are detected in the HERITAGE images.
3. We identify 45/9 matches to LMC/SMC PN candidates, 26/7 of which were classified as YSOs in alternate studies.
4. Two SNRs are detected as point sources in the HERITAGE data, SN 1987 A and SNR J052501-693842, both in the LMC. From the FIR SED of SN 1987 A, we estimate a dust mass of 0.3–1.1 $M_{\odot}$, similar to that measured by Matsuura et al. (2011) in their more detailed analysis.

Through an independent analysis, we identified ∼10,000 background galaxies in the LMC images and ∼5,000 in the SMC. These numbers are consistent with the expected number of detected background galaxies predicted by extrapolating the flux distribution of the ATLAS survey to the area of HERITAGE and applying the HERITAGE completeness curves. We estimate the resulting candidate galaxy list is contaminated by non-galaxies at 1–4%. We identified new YSOs and dust clump candidates from a subsample of the BMC for which there was ample photometric data with which to perform an independent analysis. The results of the classification can be found in the *Herschel* Science Archive tables, and Table 9 collates some statistics of the results. The primary findings are enumerated below.

1. Using a 24 μm detection as a signpost of star formation, we classified 3518 BMC sources in the LMC and 663 in the SMC as YSO candidates. Of those, 73% and 35% are newly identified YSOs in the LMC and SMC, respectively. Fewer new YSOs are identified in the SMC because its lower dust content causes the YSO population to be intrinsically dimmer in the FIR. The most likely contamination of the YSO lists is from background galaxies, but comparison with the ATLAS survey suggests that the HERITAGE probable YSOs are contaminated by background galaxies by at most 5%.
2. These new candidate YSO lists greatly expand the number of known YSOs in the MC, primarily by extending the catalogs to lower luminosities than were probed in previous studies. We estimate the HERITAGE YSO

candidate lists to be complete for young, embedded YSOs with luminosities greater than $\sim$1000 $L_{\odot}$.

3. We classified 2744 LMC and 110 SMC sources as candidate dust clumps. These sources are MC-residing FIR bright sources that lack a 24 μm counterpart in the SAGE/SAGE-SMC catalogs. The most luminous of them are massive YSOs whose mid-IR emission saturated the MIPS detector, while those less luminous are either low-luminosity YSOs not detected in the mid-IR or starless dust clumps heated by the ISRF.

Tables 8 and 9 summarize the classifications of the HERITAGE point sources based upon both our own analysis and matches to the literature. These classifications are primarily performed by analyzing the sources' photometric IR properties, however—as demonstrated here—many different objects can look photometrically similar at these wavelengths, and further follow-up investigations will need to be performed to confirm the classifications.

The authors thank the anonymous referee for comments that improved the quality of the paper. This work makes use of data collected by the *Herschel Space Observatory*. *Herschel* is an ESA space observatory with science instruments provided by European-led Principal Investigator consortia and with important participation from NASA. HIPE is a joint development by the Herschel Science Ground Segment Consortium, consisting of ESA, the NASA Herschel Science Center, and the HIFI, PACS, and SPIRE consortia. This work is based in part on observations made with the *Spitzer Space Telescope*, which is operated by the Jet Propulsion Laboratory, California Institute of Technology under a contract with NASA. We acknowledge financial support from the NASA *Herschel* Science Center, JPL contracts #1381522, #1381650, #1350371. We thank the contributions and support from the European Space Agency (ESA), the PACS and SPIRE teams, the *Herschel* Science Center (esp. L. Conversi), and the NASA *Herschel* Science Center (esp. A. Barbar and R. Paladini) and the PACS and SPIRE instrument control centers (esp. George Bendo), without which none of this work would be possible. M. Sewiło acknowledges financial support from the NASA ADAP award NNX11AG50G.

Facilities: Herschel (PACS, SPIRE), Spitzer (IRS, IRAC, MIPS)

REFERENCES

André, P., Men'shchikov, A., Bontemps, S., et al. 2010, A&A, 518, L102
Battersby, C., Bally, J., Ginsburg, A., et al. 2011, A&A, 535, A128
Beckwith, S. V. W., Sargent, A. I., Chini, R. S., & Guesten, R. 1990, AJ, 99, 924
Bernard, J.-P., Reach, W. T., Paradis, D., et al. 2008, AJ, 136, 919
Bolatto, A. D., Simon, J. D., Stanimirović, S., et al. 2007, ApJ, 655, 212
Boyer, M. L., Sargent, B., van Loon, J. T., et al. 2010, A&A, 518, L142
Boyer, M. L., Srinivasan, S., van Loon, J. T., et al. 2011, AJ, 142, 103
Carey, S. J., Noriega-Crespo, A., Mizuno, D. R., et al. 2009, PASP, 121, 76
Carlson, L. R., Sewiło, M., Meixner, M., et al. 2011, ApJ, 730, 78
Carlson, L. R., Sewiło, M., Meixner, M., Romita, K. A., & Lawton, B. 2012, A&A, 542, A66
Chandrasekhar, S. 1960, Radiative Transfer (New York: Dover)
Chen, C.-H. R., Chu, Y.-H., Gruendl, R. A., Gordon, K. D., & Heitsch, F. 2009, ApJ, 695, 511
Chen, C.-H. R., Indebetouw, R., Chu, Y.-H., et al. 2010, ApJ, 721, 1206
Chen, C.-H. R., Indebetouw, R., Muller, E., et al. 2014, ApJ, 785, 162
Churchwell, E., Babler, B. L., Meade, M. R., et al. 2009, PASP, 121, 213
Cox, A. N. 2000, Allen's Astrophysical Quantities (New York: AIP)
Cyganowski, C. J., Whitney, B. A., Holden, E., et al. 2008, AJ, 136, 2391
Diolaiti, E., Bendinelli, O., Bonaccini, D., et al. 2000, Proc. SPIE, 4007, 879
Dunham, M. M., Stutz, A. M., Allen, L. E., et al. 2014, arXiv:1401.1809
Eales, S., Dunne, L., Clements, D., et al. 2010, PASP, 122, 499
Elia, D., Schisano, E., Molinari, S., et al. 2010, A&A, 518, L97
Evans, N. J. II 1999, ARA&A, 37, 311
Ferrarotti, A. S., & Gail, H.-P. 2006, A&A, 447, 553
Galametz, M., Hony, S., Galliano, F., et al. 2013, MNRAS, 431, 1596
Galliano, F., Hony, S., Bernard, J.-P., et al. 2011, A&A, 536, A88
Gaustad, J. E., McCullough, P. R., Rosing, W., & van Buren, D. 2001, PASP, 113, 1326
Gordon, K. D., Bot, C., Muller, E., et al. 2009, ApJL, 690, L76
Gordon, K. D., Meixner, M., Meade, M. R., et al. 2011, AJ, 142, 102
Eales, S., Dunne, L., Clements, D., et al. 2010, PASP, 122, 499
Gruendl, R. A., Chu, Y.-H., Seale, J. P., et al. 2008, ApJL, 688, L9
Gruendl, R. A., & Chu, Y.-H. 2009, ApJS, 184, 172
Griffin, M. J., et al. 2010, A&A, 518, L3
Groenewegen, M. A. T., Waelkens, C., Barlow, M. J., et al. 2011, A&A, 526, A162
Habing, H. J. 1996, A&ARv, 7, 97
Hill, T., Motte, F., Didelon, P., et al. 2011, A&A, 533, A94
Hora, J. L., Cohen, M., Ellis, R. G., et al. 2008, AJ, 135, 726
Iben, I. Jr., & Renzini, A. 1983, ARA&A, 21, 271
Jørgensen, J. K., Harvey, P. M., Evans, N. J. II, et al. 2006, ApJ, 645, 1246
Kozłowski, S., & Kochanek, C. S. 2009, ApJ, 701, 508
Kozłowski, S., Onken, C. A., Kochanek, C. S., et al. 2013, ApJ, 775, 92
Mathis, J. S., Mezger, P. G., & Panagia, N. 1983, A&A, 128, 212
Matsuura, M., Dwek, E., Meixner, M., et al. 2011, Sci, 333, 1258
Mattsson, L., Höfner, S., & Herwig, F. 2007, A&A, 470, 339
Meixner, M., Gordon, K. D., Indebetouw, R., et al. 2006, AJ, 132, 2268
Meixner, M., Panuzzo, P., Roman-Duval, J., et al. 2013, AJ, 146, 62
Molinari, S., Swinyard, B., Bally, J., et al. 2010, A&A, 518, L100
Motte, F., Zavagno, A., Bontemps, S., et al. 2010, A&A, 518, L77
Muller, E., Staveley-Smith, L., Zealey, W., & Stanimirović, S. 2003, MNRAS, 339, 105
Murphy Williams, R. N., Dickel, J. R., Chu, Y., et al. 2010, BAAS, 42, 454.16
Ngeow, C., & Kanbur, S. M. 2008, ApJ, 679, 76
Oliveira, J. M., van Loon, J. T., Chen, C. -H. R., et al. 2009, ApJ, 707, 1269
Oliveira, J. M., van Loon, J. T., Sloan, G. C., et al. 2013, MNRAS, 428, 3001
Otsuka, M., van Loon, J. T., Long, K. S., et al. 2010, A&A, 518, L139
Pilbratt, G. L., et al. 2010, A&A, 518, L1
Poglitsch, A., et al. 2010, A&A, 518, L2
Rigby, E. E., Maddox, S. J., Dunne, L., et al. 2011, MNRAS, 415, 2336
Reid, W. A., & Parker, Q. A. 2006, MNRAS, 373, 521
Reid, W. A., & Parker, Q. A. 2010, MNRAS, 405, 1349
Riebel, D., Srinivasan, S., Sargent, B., & Meixner, M. 2012, ApJ, 753, 71
Romita, K. A., Carlson, L. R., Meixner, M., et al. 2010, ApJ, 721, 357
Seale, J. P., Looney, L. W., Chu, Y. -H., et al. 2009, ApJ, 699, 150
Seale, J. P., Looney, L. W., Wong, T., et al. 2012, ApJ, 751, 42
Sewiło, M., Indebetouw, R., Carlson, L. R., et al. 2010, A&A, 518, L73
Sewiło, M., Carlson, L. R., Seale, J. P., et al. 2013, ApJ, 778, 15
Shimonishi, T., Onaka, T., Kato, D., et al. 2008, ApJL, 686, L99
Shimonishi, T., Onaka, T., Kato, D., et al. 2010, A&A, 514, A12
Simon, J. D., Bolatto, A. D., Whitney, B. A., et al. 2007, ApJ, 669, 327
Sodroski, T. J., Dwek, E., Hauser, M. G., & Kerr, F. J. 1987, ApJ, 322, 101
Srinivasan, S., Meixner, M., Leitherer, C., et al. 2009, AJ, 137, 4810
Sturm, R., Drašković, D., Filipović, M. D., et al. 2013, A&A, 558, A101
Subramanian, S., & Subramaniam, A. 2009, A&A, 496, 399
Subramanian, S., & Subramaniam, A. 2010, A&A, 520, A24
Subramanian, S., & Subramaniam, A. 2012, ApJ, 744, 128
Szewczyk, O., Pietrzyński, G., Gieren, W., et al. 2009, AJ, 138, 1661
van Aarle, E., van Winckel, H., Lloyd Evans, T., et al. 2011, A&A, 530, A90
van Loon, J. T., Oliveira, J. M., Gordon, K. D., et al. 2010, AJ, 139, 68
van Loon, J. T., Oliveira, J. M., Gordon, K. D., Sloan, G. C., & Engelbracht, C. W. 2010, AJ, 139, 1553
Veneziani, M., Elia, D., Noriega-Crespo, A., et al. 2013, A&A, 549, A130
Veron-Cetty, M. P., & Veron, P. 2010, yCat, 7258, 0
Walborn, N. R., Barbá, R. H., & Sewiło, M. M. 2013, AJ, 145, 98
Werner, M. W., Roellig, T. L., Low, F. J., et al. 2004, ApJS, 154, 1
Whitney, B. A., Wood, K., Bjorkman, J. E., & Cohen, M. 2003, ApJ, 598, 1079
Whitney, B. A., Sewilo, M., Indebetouw, R., et al. 2008, AJ, 136, 18
Whitney, B. A., Robitaille, T. P., Bjorkman, J. E., et al. 2013, ApJS, 207, 30
Woods, P. M., Oliveira, J. M., Kemper, F., et al. 2011, MNRAS, 411, 1597
Zhukovska, S., & Henning, T. 2013, A&A, 555, A99